

Safe stabilization using generalized Lyapunov barrier function [★]

Jianglin Lan ^a, Eldert van Henten ^b, Peter Groot Koerkamp ^b, Congcong Sun ^{b,*}

^aJames Watt School of Engineering, University of Glasgow, Glasgow G12 8QQ, United Kingdom

^bAgricultural Biosystems Engineering Group, Wageningen University & Research, 6700 AC Wageningen, The Netherlands

Abstract

This paper addresses the safe stabilization problem, focusing on controlling the system state to the origin while avoiding entry into unsafe state sets. The current methods for solving this issue rely on smooth Lyapunov and barrier functions, which do not always ensure the existence of an effective controller even when such smooth functions are created. To tackle this challenge, we introduce the concept of a generalized (nonsmooth) Lyapunov barrier function (GenLBF), which guarantees the existence of a safe and stable controller. We outline a systematic approach for constructing a GenLBF, including a technique for efficiently computing the upper generalized derivative of the GenLBF. Using the constructed GenLBF, we propose a method for designing a piecewise continuous feedback control to achieve safe stabilization. A controller refinement strategy is further proposed to help the state trajectory escape from undesired local points occurring in systems with a special physical structure. A thorough theoretical analysis demonstrates the effectiveness of our method in addressing the safe stabilization problem for systems with single or multiple bounded unsafe state sets. Extensive simulations of linear and nonlinear systems further illustrate the efficacy of the proposed method and its superiority over the smooth control Lyapunov barrier function method.

Key words: Control barrier function, control Lyapunov function, generalized derivative, safe stabilization, nonlinear system.

1 Introduction

Stabilization, which involves steering the system state from an initial position to the origin, is a fundamental problem in control systems. Safety has also become an integral part of a control system to prevent the system from entering unsafe situations or harming other objects in the environment, especially for safety-critical systems such as aircraft (Agarwal et al., 2024), autonomous driving (Xiao et al., 2021), greenhouses (Morcego et al., 2023), and more. Therefore, it is necessary to design a feedback controller to achieve safe stabilization, aiming to stabilize the system state while avoiding entering those unsafe state sets. The safe stabilization problem is

similar to “stable while avoid” (Edwards et al., 2023).

It is well-known that the existence of a control Lyapunov function (CLF) implies that the system is asymptotically controllable to the origin (Artstein, 1983). Following this principle, the majority of literature constructs a smooth (i.e. continuous and differentiable) CLF and uses it to design a continuous feedback stabilizing control law, such as the universal control law (Sontag, 1989). In the past decade, the concept of control barrier function (CBF) (Ames et al., 2019) has been widely used to deal with system safety. The key idea of CBF for safety consists in ensuring satisfaction of an inequality constraint dependent on the derivative of CBF, so that the CBF is forward invariant. Methods for constructing a suitable CBF include optimization-based methods such as the sum-of-squares (Schneeberger et al., 2024) and convex optimization (Zhao et al., 2023), as well as learning-based methods like supervised learning (Dawson et al., 2022), reinforcement learning (Yang et al., 2023), combined learning and verification (Chen et al., 2024; Wang et al., 2023), Hamilton-Jacobi reachability analysis-based learning (Chen & Fazlyab, 2024).

To ensure both safety and stability, a common ap-

[★] This work was supported in part by the Graduate School for Production Ecology & Resource Conservation Visiting Scientist grant (037PE&RC2023), and in part by the Leverhulme Trust Early Career Fellowship (ECF-2021-517). The material in this paper was not presented at any conference.

* Corresponding author

Email addresses: jianglin.lan@glasgow.ac.uk (Jianglin Lan), eldert.vanhenten@wur.nl (Eldert van Henten), peter.grootkoerkamp@wur.nl (Peter Groot Koerkamp), congcong.sun@wur.nl (Congcong Sun).

proach is to include the separately constructed CLF and CBF(s) as constraints in an optimization problem (e.g., quadratic program) to make minimal adjustments to a provided nominal controller (Ames et al., 2016; Li et al., 2023). This approach offers design freedom but may lead to conflicts among CLF and CBFs, making the control design problem infeasible (Mestres & Cortés, 2024; Wang et al., 2024). Another mainstream approach is unifying CLF and CBF as a single scalar function. The concept of control Lyapunov barrier function (CLBF) is proposed in Romdlony & Jayawardhana (2016), utilizing a linear combination of CLF and CBF(s). The existence of a CLBF implies the existence of a closed-form continuous feedback controller, in the form of Sontag’s universal control law, to realize safe stabilization of the system. The concept of CLBF has been combined with model predictive control (Wu et al., 2019; Zheng & Zhu, 2024), sliding mode control (Gomez et al., 2022), and reinforcement learning (Du et al., 2023). Some researchers have also considered neural network-based CLBFs (Dawson et al., 2022). However, CLBF may lead to the existence of undesired local equilibrium due to cancellation between the gradients of CLF and CBF (Braun et al., 2019). Moreover, Braun & Kellett (2020) points out that in the presence of bounded unsafe state sets, the smooth CLBF (Romdlony & Jayawardhana, 2016) does not exist, and subsequently, no continuous feedback control laws can be found to achieve safe stabilization. To address this issue, the CLBF is adjusted in Wang et al. (2020) by considering the undesired stationary points as an additional unsafe state set. Nevertheless, their approach depends on identifying these undesired stationary points, which can be difficult for intricate nonlinear systems. Another attempt to unify CLF and CBF for safe stabilization is using converse Lyapunov barrier function (Meng et al., 2022), but the related theorems are not constructive.

In summary, the current mainstream methods which unify CLF and CBF as smooth functions are not applicable to a broader range of systems. This motivates the use of nonsmooth functions to unify CLF and CBF to achieve safe stabilization for a broader range of systems. The motivation for using nonsmooth CLFs to construct non-continuous stabilization feedback controllers is discussed in Sontag & Sussmann (1995) for nonlinear systems and in Liberzon (2003) for switched systems. The necessity of nonsmooth CBFs is demonstrated in Glotfelter et al. (2017), where Boolean composition of CBFs using nondifferentiable max and min operators is utilized to ensure system safety under multiple unsafe state sets. Braun et al. (2019) has made a first attempt to unify CLF and CBF via a nonsmooth function called complete control Lyapunov function (CCLF). However, their work only provides an example of constructing CCLF and deriving controller for a linear system with a single unsafe state point, while a systematic design for more general systems subject to multiple unsafe state sets still remains as an open question. Computational challenges

is another bottleneck of the existing nonsmooth functions representing CBF and CCLF. When using CLF, CBF, CLBF, and CCLF, computing their derivatives is commonly essential for evaluating their convergence and subsequently for state stabilization in the case of CLF and safety in the case of CBF, as well as safe stabilization for CLBF and CCLF. Dini derivative, a popular generalized directional derivative, is used in Glotfelter et al. (2017); Braun et al. (2019) to evaluate the convergence of CBFs and CCLF, respectively. However, as pointed by (Cortés et al., 2024), Dini derivatives are computationally challenging because: 1) Even for locally Lipschitz functions, the associated subdifferentials can sometimes be empty, 2) The subdifferential of the sum of two locally Lipschitz functions does not necessarily lie within the sum of their individual subdifferentials, and 3) The chain rule only applies when at least one of the functions is differentiable.

This paper aims to unify CLF and CBF for safe stabilization by using a nonsmooth function with easily computed generalized derivatives for implementation. The main contributions are summarized as follows:

- We propose a generalized Lyapunov barrier function (GenLBF), which can be either smooth or nonsmooth, for solving the safe stabilization problem. Compared to CLBF (Romdlony & Jayawardhana, 2016), GenLBF can avoid cancellation between the CLF and CBF gradients, and its existence is ensured in the presence of bounded unsafe sets, making it applicable for a wide range of systems.
- We develop a constructive design of GenLBF with an efficient method for assessing its appropriateness. In comparison to the CCLF construction (Braun et al., 2019), our design is based on the upper generalized derivative that is computationally simpler and applicable to multiple unsafe state sets.
- Based on the GenLBF, we propose a systematic method for designing a piecewise continuous feedback controller to ensure safe stabilization. Compared to Braun et al. (2019), our control design works for both linear and Lipschitz control-affine nonlinear systems.
- We propose a controller refinement strategy to assist the system in escaping from undesired local points, particularly for systems with specific structures like the simple mobile robot modeled by a double integrator. However, when utilizing the CLBF method (Romdlony & Jayawardhana, 2016) the system is unable to escape from these undesired local points.

The remainder of the paper is structured as follows: Section 2 describes the problem with some useful concepts. Section 3 presents the proposed GenLBF design. Section 4 introduces a GenLBF-based control design and a control refinement to handle systems with special structures, which are directly extended to manage multiple unsafe sets as illustrated in Section 5. Section 6 provides the simulation results. Section 7 draws the conclusions.

Notation: The symbol \mathbb{R}^n is the n -dimensional Euclidean space and $\mathbb{R}_{\geq 0}$ is the set of non-negative real numbers. For $x, y \in \mathbb{R}^n$, $\|x\|$ is the 2-norm and $\langle x, y \rangle = x^\top y$. For a vector $y \in \mathbb{R}^{1 \times m}$, $\mu(y) = y^\top / \|y\|^2$ and $\bar{\mu}(y) = [\mu(y_1), \dots, \mu(y_m)]^\top$. \mathcal{O} is an open set, while $\bar{\mathcal{O}}$ is its closure. For a function $h(x) : \mathcal{D} \mapsto \mathbb{R}$, $\mathcal{D} \subseteq \mathbb{R}^n$, if h is continuously differentiable, we denote its gradient by $\nabla h(x)$ and write $\dot{h}(x) = \nabla h(x)\dot{x}$; if h is non-differentiable, we use $\partial h(x)$ to represent its generalized gradient set. If \mathcal{S} is a set, $\partial \mathcal{S}$ represents its boundary. A continuous function $\rho : \mathbb{R}_{\geq 0} \mapsto \mathbb{R}_{\geq 0}$ is of class- \mathcal{P} if $\rho(0) = 0$, and $\rho(s) > 0, \forall s > 0$. A function $\alpha \in \mathcal{P}$ is of class- \mathcal{K} if it is strictly increasing and is of class- \mathcal{K}_∞ if additionally $\lim_{s \rightarrow \infty} \alpha(s) = \infty$. A continuous function $\rho : \mathbb{R}_{\geq 0} \mapsto \mathbb{R}_{\geq 0}$ is of class- \mathcal{L} if it is strictly decreasing and $\lim_{s \rightarrow \infty} \rho(s) = 0$. A continuous function $\beta : \mathbb{R}_{\geq 0}^2 \mapsto \mathbb{R}_{\geq 0}$ is of class- \mathcal{KL} if $\beta(\cdot, s) \in \mathcal{K}_\infty, \forall s \in \mathbb{R}_{\geq 0}$ and $\beta(s, \cdot) \in \mathcal{L}, \forall s \in \mathbb{R}_{\geq 0}$.

2 Problem description and basic concepts

Consider a class of continuous-time control-affine system

$$\dot{x} = f(x) + g(x)u \quad (1)$$

with the state $x \in \mathbb{R}^n$, control input $u \in \mathbb{R}^m$, and nonlinear functions $f(x) \in \mathbb{R}^n$ and $g(x) \in \mathbb{R}^{n \times m}$. We denote $\mathcal{X} \subset \mathbb{R}^n$ as the operational state space and $\mathcal{F}(x)$ as the set of solutions to (1) starting at the initial state $x(0)$. To simplify notations, we will express the system (1) as $\dot{x} = F(x, u)$ and more compactly as $\dot{x} = F(x)$ under a state-feedback controller $u = \kappa(x)$.

Assumption 2.1 *The functions $f(x)$ and $g(x)$ are locally Lipschitz continuous, $f(0) = 0$, $g(x)$ has full rank m , and the origin $x = 0$ is the desired equilibrium of (1).*

This assumption is widely used in the existing works about continuous-time control-affine systems, including those consider CBF (Ames et al., 2019), CLBF (Romdlony & Jayawardhana, 2016) and CCLF (Braun et al., 2019). The type of systems in (1) under Assumption 2.1 can represent many real-world control systems such as robot manipulators (Zeng et al., 2023), aircraft (Agarwal et al., 2024), autonomous vehicles (Xiao et al., 2021), and nonholonomic mobile robots (Marley et al., 2024).

This work aims to design a feedback controller (see Section 4) to achieve safe stabilization of system (1) in the sense of \mathcal{KL} -stability and safety (Braun et al., 2021).

Definition 2.1 (*\mathcal{KL} -stability & safety*) *Consider the system $\dot{x} = F(x, u)$ with the state space $\mathcal{X} \subset \mathbb{R}^n$ and an unsafe state set $\mathcal{O} \subset \mathcal{X}$ satisfying $0 \notin \mathcal{O}$. This system is \mathcal{KL} -stable w.r.t. the origin and never enters \mathcal{O} if there exists a feedback controller $u = \kappa(x)$ such that for all the*

initial state $x(0) \in \mathcal{X} \setminus \mathcal{O}$,

$$\|x(t)\| \leq \beta(\|x(0)\|, t), \quad x(t) \notin \mathcal{O}, \quad \forall t \geq 0,$$

where β is a \mathcal{KL} function.

According to Definition 2.1, $\lim_{\|x(0)\| \rightarrow 0} \beta(\|x(0)\|, t) = 0$ and $\lim_{t \rightarrow \infty} \beta(\|x(0)\|, t) = 0$. Hence, given a finite $x(0)$, deviation from the origin $\|x(t)\|$ is bounded for all $t \geq 0$ and asymptotically stable, i.e. $\lim_{t \rightarrow \infty} \|x(t)\| = 0$.

The control design in this paper is based on a generalized nonsmooth Lyapunov barrier function (GenLBF) to be presented in Section 3. Evaluating convergence (decreasing condition) of the nonsmooth GenLBF requires using the concept of generalized derivative.

Definition 2.2 (*Generalized derivative*) *Let $h : \mathcal{D} \mapsto \mathbb{R}$, $\mathcal{D} \subseteq \mathbb{R}^n$, be a locally Lipschitz continuous function with dependence on (x, u) and $\mathcal{F} : \mathbb{R}^n \times \mathbb{R}^m \mapsto \mathbb{R}^n$ be a set-valued map. The upper generalized derivative $\bar{M}_{\mathcal{F}}h(x, u)$ and lower generalized derivative $\underline{M}_{\mathcal{F}}h(x, u)$ of h w.r.t. \mathcal{F} at (x, u) are defined as*

$$\bar{M}_{\mathcal{F}}h(x, u) = \sup L_{\mathcal{F}}h(x, u), \quad \underline{M}_{\mathcal{F}}h(x, u) = \inf L_{\mathcal{F}}h(x, u),$$

where $L_{\mathcal{F}}h(x, u) = \{\langle \xi, v \rangle \in \mathbb{R} \mid v \in \mathcal{F}(x, u), \xi \in \partial h(x)\}$ is the set-valued Lie derivative. Moreover, when $\bar{M}_{\mathcal{F}}h(x, u) = \underline{M}_{\mathcal{F}}h(x, u)$, h is said to be generalized differentiable w.r.t. \mathcal{F} with the generalized derivative $M_{\mathcal{F}}h(x, u) = \bar{M}_{\mathcal{F}}h(x, u) = \underline{M}_{\mathcal{F}}h(x, u)$.

Definition 2.2 is adapted from the Mandalay derivative (Cortes et al., 2024). When h is locally Lipschitz and \mathcal{F} is compact, $L_{\mathcal{F}}h(x, u)$ is compact and nonempty, while $\bar{M}_{\mathcal{F}}h(x, u)$ and $\underline{M}_{\mathcal{F}}h(x, u)$ are finite. If \mathcal{F} is a singleton f and h is continuously differentiable, the generalized derivative is the usual derivative and can be expressed in Lie derivative notation as $M_{f}h(x, u) = L_{f}h(x, u)$. If there is no explicit dependence on u , $M_{\mathcal{F}}h(x, u)$ and $\mathcal{F}(x, u)$ will simply be denoted as $M_{\mathcal{F}}h(x)$ and $\mathcal{F}(x)$, respectively. As shown in Cortes et al. (2024), the generalized derivative employed in this paper is computationally easier than the Dini derivative used in the literature for evaluating convergence of the nonsmooth CCLF (Braun et al., 2019) or nonsmooth CBF (Glotsfelter et al., 2017). More details of how to compute the generalized derivative will be provided in Section 3.

The concept of regular function (Clarke, 1990) is needed for computing the generalized derivative.

Definition 2.3 (*Regular function*) *A locally Lipschitz continuous function $f : \mathbb{R}^n \mapsto \mathbb{R}$ is said to be regular at x if for all $v \in \mathbb{R}^n$, $f^\circ(x; v) = f'(x; v)$, where $f^\circ(x; v) = \limsup_{y \rightarrow x, t \downarrow 0} \frac{f(y+tv) - f(y)}{t}$ is the generalized direc-*

tional derivative and $f'(x;v) = \lim_{t \downarrow 0} \frac{f(x+tv) - f(x)}{t}$ is the one-sided directional derivative.

3 Generalized Lyapunov barrier function

3.1 Definition and evaluation of GenLBF

Definition 3.1 (GenLBF) Consider the system $\dot{x} = F(x)$ with the state space \mathcal{X} , desired equilibrium $x_g = 0$, and disjoint unsafe state sets $\mathcal{O}_i \subset \mathcal{X}$, $i \in [1, N]$, satisfying $x_g \notin \mathcal{O} := \cup_{i=1}^N \mathcal{O}_i$. A Lipschitz continuous function $V(x) : \mathbb{R}^n \mapsto \mathbb{R}$ is a generalized Lyapunov barrier function for this system, if there exist functions $\alpha_1, \alpha_2 \in \mathcal{K}_\infty$ and $\rho \in \mathcal{P}$, and constants $c_i > 0$, $i \in [1, N]$, such that

$$V(x) = c_i, \forall x \in \partial \mathcal{O}_i, \quad c_i \leq \min_{x \in \mathcal{O}_i} V(x), \quad i \in [1, N], \quad (2a)$$

$$\alpha_1(\|x - x_g\|) \leq V(x) \leq \alpha_2(\|x - x_g\|), \quad \forall x \in \mathcal{X}, \quad (2b)$$

$$\overline{M}_{\mathcal{F}}V(x) \leq -\rho(\|x\|), \quad \forall x \in \mathcal{X} \setminus (\mathcal{O} \cup \{x_g\}). \quad (2c)$$

Condition (2a) indicates that the level-set $V(x) = c_i$ separates the state trajectory from each unsafe set \mathcal{O}_i , $i \in [1, N]$. Condition (2b) ensures that $V(x)$ is positive definite except at $x = x_g$, radially unbounded, and $V(x_g) = 0$. Under (2a) and (2b), $V(x)$ carries the properties of a CBF and a CLF, respectively. Furthermore, (2c) ensures that $V(x)$ is decreasing for all $x \in \mathcal{X} \setminus (\mathcal{O} \cup x_g)$ and thus converges to $V(x_g) = 0$.

Compared to the existing concept of CCLF (Braun et al., 2019, Definition 3) for safe stabilization, GenLBF considers a bounded state space \mathcal{X} instead of full space \mathbb{R}^n , a generic desired equilibrium $x = x_g$ instead of the origin $x = 0$, and using the upper generalized derivative in (2c) instead of the hard to compute Dini derivative. Using the generic equilibrium x_g keeps generalizability of Definition 3.1, which obviously contains $x_g = 0$ as a special scenario. The decreasing condition (2c) is based on the upper generalized derivative $\overline{M}_{\mathcal{F}}V(x)$, instead of the generalized derivative $M_{\mathcal{F}}V(x)$, because the former always exists while the latter exists only when $\overline{M}_{\mathcal{F}}V(x) = \underline{M}_{\mathcal{F}}V(x)$, as shown in Definition 2.2. By using the upper generalized derivative, satisfaction of (2c) always implies satisfaction of $M_{\mathcal{F}}V(x) \leq -\rho(\|x\|)$, $\forall x \in \mathcal{X} \setminus (\mathcal{O} \cup x_g)$.

We show in Theorem 3.1 that existence of a GenLBF is sufficient to certify \mathcal{KL} -stability and safety of the system.

Theorem 3.1 Consider the system $\dot{x} = F(x)$ with the state space \mathcal{X} , desired equilibrium $x_g = 0$, and disjoint unsafe state sets $\mathcal{O}_i \subset \mathcal{X}$, $i \in [1, N]$, satisfying $x_g \notin \mathcal{O} := \cup_{i=1}^N \mathcal{O}_i$. This system is \mathcal{KL} -stable and safe if $V(x)$ is a GenLBF for it and $x(0) \in \mathcal{X}_0 \subseteq \mathcal{X} \setminus \mathcal{O}$.

Proof. The proof of Theorem 3.1 is adapted from that of (Braun et al., 2019, Theorem 2). Under (2a), we define

the set-value map $H : \mathbb{R}_{\geq 0} \mapsto \mathbb{R}^n$ as

$$H(v) = \{x \in \mathcal{X} \mid V(x) = v\}, \quad (3)$$

and the function $\tilde{\gamma} : \mathbb{R}_{\geq 0} \mapsto \mathbb{R}_{\geq 0}$ as

$$\tilde{\gamma}(v) = \min\{\rho(\|x\|) \mid x \in H(v) \setminus (\mathcal{O} \cup x_g)\}. \quad (4)$$

According to (2b), $\rho \in \mathcal{P}$ and $V(x) > 0$ for all $x \neq x_g$, thus $\tilde{\gamma}(v) > 0, \forall v \neq 0$ and $\tilde{\gamma}(V(x_g)) = 0$. We further define $\gamma \in \mathcal{P}$ such that $\gamma(v) \leq \tilde{\gamma}(v), \forall v \in \mathbb{R}_{\geq 0}$. According to (3) and (4), $\gamma(v) \leq \tilde{\gamma}(v) \leq \rho(\|x\|)$.

Let $\phi(\cdot; x) : \mathbb{R}_{\geq 0} \mapsto \mathbb{R}^n$ be a solution of $\dot{x} = F(x)$, i.e. $\phi(\cdot; x) \in \mathcal{F}(x)$. Since $V(x)$ is locally Lipschitz, $V(\phi(\cdot; x))$ is absolutely continuous, i.e. differentiable almost everywhere. For each $x \in \mathcal{X} \setminus \mathcal{O}$, we assume that there exists a solution $\phi(\cdot; x) \in \mathcal{F}(x)$ such that for almost all $t \in \mathbb{R}_{\geq 0}$,

$$\frac{d}{dt}V(\phi(t; x)) \leq -\frac{1}{4}\rho(\|\phi(t; x)\|) \leq -\frac{1}{4}\gamma(V(\phi(t; x))), \quad (5)$$

where the last inequality is obtained by substituting $v = V(\phi(t; x))$ and $x = \phi(t; x)$ into $\gamma(v) \leq \rho(\|x\|)$.

If condition (2b) is satisfied, $\alpha_1(\|x - x_g\|) \leq V(x) \leq \alpha_2(\|x - x_g\|)$ where $x_g = 0$. We then have

$$V(\phi(t; x)) \geq \alpha_1(\|\phi(t; x)\|) \Rightarrow \|\phi(t; x)\| \leq \alpha_1^{-1} \circ V(\phi(t; x)),$$

where \circ represents function composition.

By applying the comparison principle (Sontag & Wang, 2000), there exists a function $\beta \in \mathcal{KL}$ such that $V(\phi(t; x)) \leq \beta(V(x), t)$ and thus

$$\begin{aligned} \|\phi(t; x)\| &\leq \alpha_1^{-1} \circ V(\phi(t; x)) \leq \alpha_1^{-1} \circ \beta(V(x), t) \\ &\leq \alpha_1^{-1} \circ \beta(\alpha_2(\|x\|), t) \\ &= \tilde{\beta}(\|x\|, t) \end{aligned}$$

with the function $\tilde{\beta} \in \mathcal{KL}$. By Definition 2.1, this concludes that system $\dot{x} = F(x)$ is \mathcal{KL} -stable and safe.

The above proof relies on the assumption that there exists a solution $\phi(\cdot; x) \in \mathcal{F}(x)$ such that for almost all $t \in \mathbb{R}_{\geq 0}$, (5) holds. To complete the proof, we use the contradiction method to show that this assumption is satisfied under (2c).

We assume that there exists $x \in \mathcal{X} \setminus (\mathcal{O} \cup x_g)$ and a constant T such that all solutions $\phi(\cdot; x) \in \mathcal{F}(x)$ satisfy

$$\frac{d}{dt}V(\phi(t; x)) > -\frac{1}{4}\rho(\|\phi(t; x)\|), \quad \forall t \in [0, T]. \quad (6)$$

If (2c) holds, there exists $\tilde{w} \in F(x)$ such that

$$\overline{M}_{\mathcal{F}}V(x) \leq -\rho(\|x\|). \quad (7)$$

Since $F(x)$ is Lipschitz continuous, there is a Lipschitz continuous function $w : [0, T] \mapsto \mathbb{R}^n$ such that $\phi(\cdot; x) \in \mathcal{F}(x)$ and $\dot{\phi}(t; x) = w(t)$ for almost all $t \in [0, T]$ and $w(0) = \tilde{w}$. Note that $\phi(\cdot; x)$ is also Lipschitz continuous. By choosing $\epsilon > 0$ such that $\rho(y)/2 < \rho(\|x\|), \forall y \in \mathcal{B}_\epsilon(x) \setminus (\mathcal{O} \cup x_g)$ where $\mathcal{B}_\epsilon(x) := \{y \in \mathbb{R}^n \mid \|y - x\| < \epsilon\}$, then $\frac{1}{2}\rho(\|\phi(t; x)\|) < \rho(\|x\|)$ and $-\rho(\|\phi(t; x)\|) > -2\rho(\|x\|)$. Hence, (6) leads to

$$\begin{aligned} V(\phi(t; x)) - V(\phi(0; x)) &> -\rho(\|\phi(t; x)\|)/4 \\ &> -\rho(\|x\|)/2 > -\rho(\|x\|), \end{aligned} \quad (8)$$

for all $t \in [0, T]$ such that $\phi(t; x) \in \mathcal{B}_\epsilon(x) \setminus (\mathcal{O} \cup x_g)$. Since the left-most part of (8) is Lipschitz continuous, taking the limit inferior for $t \rightarrow 0$ on both sides of (8) to obtain $dV(x; \phi(t; x)) > -\rho(\|x\|)$. This leads to a contradiction with (7) and thus the assumption (6) is invalid. This confirms validity of (5) and thus completes the proof. \square

Computing the left-hand side of (2c) can be challenging because $\overline{M}_{\mathcal{F}}V(x)$ is a nonlinear operator depending on $V(x)$. Inspired by Cortes et al. (2024), an efficient computation method for obtaining $\overline{M}_{\mathcal{F}}V(x)$ is expressing $V(x)$ as a composite function with simpler components and bound it based on the generalized derivative of the simpler components. The computation method relies on using the chain rule and the superposition rule (for linear combination of functions) in Theorem 3.2, Corollary 3.1, and Theorem 3.3. These results are adapted from Theorem 1, Corollary 1, Lemma 2 and Theorem 2 in Cortes et al. (2024) by considering the upper Mandalay derivative, instead of lower Mandalay derivative. The associated proofs are adapted from those in Cortes et al. (2024) and provided in the appendix for completion.

Theorem 3.2 (Chain rule) *Consider the composite function $h(x) = h_1(h_2(x))$, where $h_1 : \mathbb{R} \mapsto \mathbb{R}$ and $h_2 : \mathcal{D} \mapsto \mathbb{R}, \mathcal{D} \subseteq \mathbb{R}^n$, are locally Lipschitz functions. If $\mathcal{F} : \mathbb{R}^n \times \mathbb{R}^m \mapsto \mathbb{R}^n$ is a set-valued map and takes only nonempty, compact and convex values, then $\forall x \in \mathcal{D}$,*

$$\begin{aligned} \overline{M}_{\mathcal{F}}h(x, u) \leq \max\{ &\underline{M}_{\mathcal{F}}h_2(x, u) \cdot \underline{\partial}h_1(h_2(x)), \\ &\underline{M}_{\mathcal{F}}h_2(x, u) \cdot \overline{\partial}h_1(h_2(x)), \\ &\overline{M}_{\mathcal{F}}h_2(x, u) \cdot \underline{\partial}h_1(h_2(x)), \\ &\overline{M}_{\mathcal{F}}h_2(x, u) \cdot \overline{\partial}h_1(h_2(x))\}. \end{aligned} \quad (9)$$

The equality holds if \mathcal{F} is a singleton, h_2 is continuously differentiable, and h_1 is regular.

Proof. See Appendix A. \square

When h_2 is generalized differentiable, $\overline{M}_{\mathcal{F}}h_2(x, u) = \underline{M}_{\mathcal{F}}h_2(x, u) = M_{\mathcal{F}}h_2(x, u)$ and thus (9) becomes $\overline{M}_{\mathcal{F}}h(x, u) \leq \max\{M_{\mathcal{F}}h_2(x, u) \cdot \underline{\partial}h_1(h_2(x)), M_{\mathcal{F}}h_2(x, u) \cdot \overline{\partial}h_1(h_2(x))\}, \forall x \in \mathcal{D}$. By considering the cases $M_{\mathcal{F}}h_2(x, u) \geq 0$ and $M_{\mathcal{F}}h_2(x, u) < 0$, Corollary 3.1 follows from Theorem 3.2.

Corollary 3.1 *In Theorem 3.2, if h_2 is generalized differentiable, then $\forall x \in \mathcal{D}$,*

$$M_{\mathcal{F}}h(x, u) \leq \begin{cases} M_{\mathcal{F}}h_2(x, u) \cdot \overline{\partial}h_1(h_2(x)), & M_{\mathcal{F}}h_2(x, u) \geq 0 \\ M_{\mathcal{F}}h_2(x, u) \cdot \underline{\partial}h_1(h_2(x)), & \text{otherwise} \end{cases}.$$

Theorem 3.3 (Superposition rule) *Consider the function $h = \sum_{i=1}^N \lambda_i h_i$ with constants $\lambda_i > 0, i \in I^p \subseteq \{1, \dots, N\}$, and $\lambda_i < 0, i \in I^n = \{1, \dots, N\} \setminus I^p$, and locally Lipschitz functions $h_i : \mathcal{D} \mapsto \mathbb{R}, \mathcal{D} \subseteq \mathbb{R}^n, i \in [1, N]$. If $\mathcal{F} : \mathbb{R}^n \times \mathbb{R}^m \mapsto \mathbb{R}^n$ is a set-valued map and takes only nonempty, compact and convex values, then $\forall x \in \mathcal{D}$,*

$$\overline{M}_{\mathcal{F}}h(x, u) \leq \sum_{i \in I^p} \lambda_i \overline{M}_{\mathcal{F}}h_i(x, u) + \sum_{i \in I^n} \lambda_i \underline{M}_{\mathcal{F}}h_i(x, u). \quad (10)$$

The equality holds if \mathcal{F} is a singleton, I^n is empty, and $h_i, i \in [1, N]$, are regular.

Proof. See Appendix B. \square

3.2 Constructive design of GenLBF

This section illustrates the key idea of constructing a suitable GenLBF by considering a single set of unsafe states. A direct extension of the method to handle multiple sets of unsafe states will be described in Section 5.

We consider that the unsafe states are enclosed by an open n -ball \mathcal{O} defined by

$$\mathcal{O} = \{x \in \mathcal{X} \setminus \{0\} \mid \|x - x_c\| < \sqrt{r}\}, \quad (11)$$

where x_c is the centre and \sqrt{r} is the radius. The enclosure of \mathcal{O} is denoted as $\overline{\mathcal{O}}$. Without loss of generality, we can always find an open n -ball \mathcal{O} to enclose the bounded unsafe state region with an arbitrary shape. The use of n -ball may lead to a conservative control law for ensuring safe stabilization, but it facilitates illustration of the proposed method. Using a less conservative set representation of the unsafe states is left for future investigation. Theorem 3.4 presents a way for constructing a GenLBF.

Theorem 3.4 *Consider the system $\dot{x} = F(x)$ under Assumption 4.1 with the state space $\mathcal{X} \subset \mathbb{R}^n$ and an unsafe state set \mathcal{O} in (11). This system is \mathcal{KL} -stable and safe for all $x(0) \in \mathcal{X} \setminus (\mathcal{O} \cup \mathcal{R}_1 \cup \mathcal{R}_3)$ if*

- 1) *The GenLBF $V(x)$ is constructed as*

$$\begin{aligned} V(x) &= \max(L(x), B(x)), \\ L(x) &= \|x\|^2, \quad B(x) = \eta_2 - \eta_1 \|x - x_c\|^2, \end{aligned} \quad (12)$$

with the design constants η_1 and η_2 satisfying

$$\begin{aligned} \eta_1 &\geq (\|x_c\| + \sqrt{r}) / (\|x_c\| - \sqrt{r}), \\ \eta_2 &= \eta_1 r + \max_{x \in \overline{\mathcal{O}}} L(x) + w, \end{aligned} \quad (13)$$

where $0 < w < \eta_1(\|x_c\|^2 - r) - (\|x_c\| + \sqrt{r})^2$.
2) There exists a function $\rho(\|x\|) \in \mathcal{P}$ such that

$$\overline{M}_{\mathcal{F}}V(x) \leq -\rho(\|x\|), \quad (14)$$

with $\overline{M}_{\mathcal{F}}V(x)$ in the form of

$$\overline{M}_{\mathcal{F}}V(x) = d_i(x), \quad x \in \mathcal{R}_i, \quad i \in [1, 3], \quad (15)$$

where $d_1(x) = P(x)F(x)$, $d_2(x) = 2x^\top F(x)$,
 $d_3(x) = 0.5(d_1(x) + d_2(x)) + 0.5|d_1(x) - d_2(x)|$,
 $P(x) = -2\eta_1(x - x_c)^\top$, and

$$\begin{aligned} \mathcal{R}_1 &= \{x \in \mathcal{X} \mid B(x) > L(x), x \notin \mathcal{O}\}, \\ \mathcal{R}_2 &= \{x \in \mathcal{X} \mid B(x) < L(x)\}, \\ \mathcal{R}_3 &= \{x \in \mathcal{X} \mid B(x) = L(x)\}. \end{aligned} \quad (16)$$

Proof. For all $x \in \mathcal{O}$, it holds that $0 \leq \|x - x_c\|^2 < r$, which leads to $\eta_2 - \eta_1 r < \eta_2 - \eta_1 \|x - x_c\|^2 \leq \eta_2$ and thus $\eta_2 - \eta_1 r < B(x) \leq \eta_2, \forall x \in \mathcal{O}$. By the design of η_2 in (13), $\eta_2 - \eta_1 r \geq \max_{x \in \overline{\mathcal{O}}} L(x)$. Then we have $B(x) > L(x), \forall x \in \mathcal{O}$ and $B(x) \neq L(x), \forall x \in \mathcal{O}$. Subsequently, $V(x) = \max(L(x), B(x)) = B(x), \forall x \in \mathcal{O}$. Therefore, there is a positive constant $c = \eta_2 - \eta_1 r$ such that $V(x)$ satisfies the condition (2a). To complete the proof of (2a), we also need to ensure that the desired equilibrium 0 is outside of the region $B(x) \leq L(x)$, i.e. $B(0) < L(0)$. Since \mathcal{O} is a n -ball, $\max_{x \in \overline{\mathcal{O}}} L(x) = \max_{x \in \overline{\mathcal{O}}} \|x\|^2 = (\|x_c\| + \sqrt{r})^2$. According to (13), we can derive that $\eta_2 < \eta_1 \|x_c\|^2$ and thus $\eta_2 - \eta_1 \|x_c\|^2 < 0$. This confirms that $B(0) < L(0)$.

Since $V(x)$ is in the form of (12), (2b) is satisfied by defining the \mathcal{K}_∞ functions $\alpha_1(\|x\|) = \|x\|^2$ and $\alpha_2(\|x\|) = \|x\|^2 + \max_{\|y\| \leq \|x\|} V(y)$.

To verify condition (2c), we rearrange $V(x)$ into

$$V(x) = h_0(x) + h_1(h_2(x)),$$

where $h_0(x) = 0.5(B(x) + L(x))$, $h_1(h_2(x)) = 0.5|h_2(x)|$, and $h_2(x) = B(x) - L(x)$. Note that both $h_0(x)$ and $h_2(x)$ are continuously differentiable, while $h_1(h_2)$ is non-differentiable at $h_2(x) = 0$ but locally Lipschitz in \mathcal{X} . Hence, we need to derive the generalized derivative of $V(x)$ in the three state regions defined in (16).

1) *Region \mathcal{R}_1 :* In this case, $h_2(x) > 0$ and $h_1(h_2(x)) = h_2(x) = B(x) - L(x)$. Thus, $V(x) = B(x)$ which is continuously differentiable with the generalized derivative

$$M_{\mathcal{F}}V(x) = \dot{B}(x) = P(x)F(x),$$

where $P(x) = -2\eta_1(x - x_c)^\top$.

2) *Region \mathcal{R}_2 :* In this case, $h_2(x) < 0$ and $h_1(h_2(x)) = 0.5(L(x) - B(x))$. Thus, $V(x) = L(x)$ which is continuously differentiable with the generalized derivative

$$M_{\mathcal{F}}V(x) = \dot{L}(x) = 2x^\top F(x).$$

3) *Region \mathcal{R}_3 :* In this case, $h_2(x) = 0$ and $V(x)$ is non-differentiable. At the points where $h_2(x) = 0$, we derive

$$\begin{aligned} \partial h_1 &= \begin{cases} -0.5, & h_2(x) \rightarrow 0^- \\ 0.5, & h_2(x) \rightarrow 0^+ \end{cases}, \\ \partial h_2 &= \nabla h_2(x) = P(x) - 2x^\top, \\ \partial h_0 &= \nabla h_0(x) = 0.5(P(x) + 2x^\top). \end{aligned}$$

Since $h_2(x)$ is generalized differentiable, $M_{\mathcal{F}}h_2(x) = \dot{h}_2(x)$. By using Corollary 3.1, it holds that

$$M_{\mathcal{F}}(h_1(h_2))(x) \leq \begin{cases} 0.5\dot{h}_2(x), & \dot{h}_2(x) \geq 0 \\ -0.5\dot{h}_2(x), & \dot{h}_2(x) < 0 \end{cases}.$$

This is equivalent to $M_{\mathcal{F}}(h_1(h_2))(x) \leq 0.5|\dot{h}_2(x)|$. Therefore, by using the superposition rule in Theorem 3.3, the generalized derivative of $V(x)$ when $B(x) = L(x)$ is derived as

$$\begin{aligned} M_{\mathcal{F}}V(x) &= \dot{h}_0(x) + M_{\mathcal{F}}(h_1(h_2))(x) \\ &\leq \dot{h}_0(x) + 0.5|\dot{h}_2(x)| \\ &= 0.5(P(x) + 2x^\top)F(x) + 0.5|(P(x) - 2x^\top)F(x)|. \end{aligned}$$

Combining the three cases leads to the upper generalized derivative of $V(x)$ in (15). Hence, if there exists a function $\rho(\|x\|) \in \mathcal{P}$ such that $\overline{M}_{\mathcal{F}}V(x) \leq -\rho(\|x\|)$ in all the three state regions, then the condition (2c) is satisfied.

Note that $0 \in \mathcal{R}_2$ and $V(x) = L(x)$ in the region \mathcal{R}_2 . Hence when $x = 0$, $V(0) = 0$ and $M_{\mathcal{F}}V(x) = 0$, meaning that once arriving at the origin x will remain there. Therefore, the condition (2c) is satisfied for all $x \in \mathcal{X} \setminus \mathcal{O}$. In summary, the above shows that the GenLBF $V(x)$ satisfies all the conditions in Definition 3.1, thus according to Theorem 3.1, the system is safe and \mathcal{KL} -stable under Definition 2.1 for all $x(0) \in \mathcal{X} \setminus \mathcal{O}$. \square

3.3 Properties of the constructed GenLBF

1) *Buffer width.* For the proposed GenLBF (12), the points satisfying $x \in \mathcal{R}_3$, i.e. $B(x) = L(x)$, are on the sphere \mathcal{S} described by

$$\|x - \bar{x}_c\|^2 = \bar{r} \quad (17)$$

with the centre $\bar{x}_c = \eta_1 x_c / (1 + \eta_1)$ and radius $\sqrt{\bar{r}}$ satisfying $\bar{r} = [(1 + \eta_1)\eta_2 - \eta_1 \|x_c\|^2] / (1 + \eta_1)^2$. Further notice

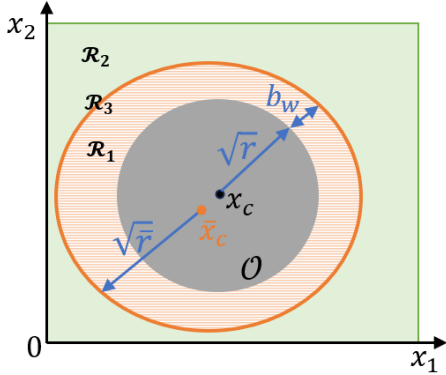


Fig. 1. A simple 2-D graphic illustration of the proposed GenLBF design. The state regions \mathcal{R}_1 , \mathcal{R}_2 and \mathcal{R}_3 are defined in (16). \sqrt{r} is the radius of unsafe boundary $\partial\mathcal{O}$ centred at x_c , $\sqrt{\bar{r}}$ is the radius of \mathcal{R}_3 ($B(x) = L(x)$) centred at \bar{x}_c , and b_w (buffer width) is the shortest distance between these two boundaries.

that the distance between the two centres x_c and \bar{x}_c is $\|x_c - \bar{x}_c\| = \|x_c\|/(1 + \eta_1)$. We can then rewrite \bar{r} in the form of

$$\bar{r} = \left(\sqrt{r} + \frac{\|x_c\|}{1 + \eta_1} \right)^2 + b_w^2 \quad (18)$$

with $b_w = \sqrt{w/(\eta_1 + 1)}$. The variable b_w represents the shortest distance between the boundaries \mathcal{R}_3 and $\partial\mathcal{O}$, which is regarded as the buffer width. We can design the parameters η_1 and w to tune the buffer width. Figure 1 provides a simple 2-D graphic illustration of the proposed GenLBF design.

The smooth CLBF (Romdlony & Jayawardhana, 2016) linearly combines CLF and CBF, leading to existence of undesired local equilibrium due to cancellation between the gradients of CLF and CBF. The proposed GenLBF (12) uses the max operation, guaranteeing that 0 is the strict global minimum. Theorem 3.4 offers a systematic way for constructing a suitable GenLBF to certify \mathcal{KL} -stability and safety of an autonomous system $\dot{x} = F(x)$. This result will be used in Section 4 for designing a feedback controller to ensure safe stabilization of the non-autonomous system (1).

2) *Shrunk state region \mathcal{R}_3 .* As shown in (15) and (16), the upper generalized derivative $\overline{\mathcal{M}}_{\mathcal{F}}V(x)$ for $x \in \mathcal{R}_3$ involves the absolute operator. This imposes challenges in finding the function $\rho(\|x\|)$ to evaluate the decreasing condition (14), especially for the control design to be described later. In this section, we show that the state region \mathcal{R}_3 to evaluate can be shrunk, which can ease evaluating the decreasing condition in this region. Proposition 3.1 shows that \mathcal{R}_3 can be shrunk to a smaller set to facilitate evaluation, whose key idea is graphically demonstrated in Fig. 2.

Proposition 3.1 *For the GenLBF constructed in Theorem 3.4, the state region \mathcal{R}_3 can be shrunk as $\mathcal{R}_3 \setminus \hat{\mathcal{R}}_3$*

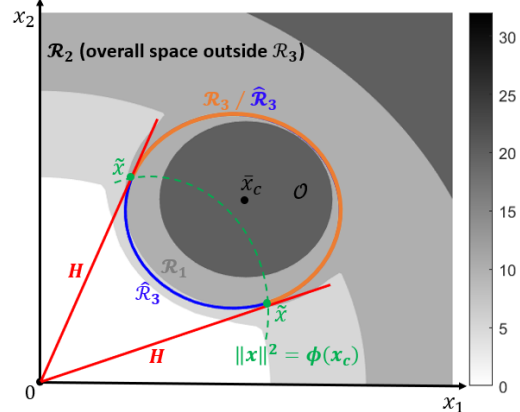


Fig. 2. A simple 2-D graphic illustration of the idea of shrinking the region \mathcal{R}_3 (represented by the sphere $\|x - \bar{x}_c\|^2 = \bar{r}$) by removing the part $\hat{\mathcal{R}}_3 = \{x \in \mathcal{R}_3 \mid \|x\|^2 < \phi(x_c)\}$. The greyscale (where darker means bigger value) indicates the different values of the GenLBF $V(x)$ in the state space $\mathcal{X} := \mathcal{R}_2 \cup \mathcal{R}_3 \cup \mathcal{R}_1 \cup \mathcal{O}$. The regions \mathcal{R}_1 , \mathcal{R}_2 and \mathcal{R}_3 are defined in (16). H represents a tangent plane of the sphere at \tilde{x} .

with the removed subset

$$\hat{\mathcal{R}}_3 = \{x \in \mathcal{R}_3 \mid \|x\|^2 < \phi(x_c)\}, \quad (19)$$

where $\phi(x_c) = (\eta_1\|x_c\|^2 - \eta_2)/(\eta_1 + 1)$. Moreover, $\hat{\mathcal{R}}_3$ is not a limit cycle for the state trajectory.

Proof. With regard to the sphere \mathcal{S} in (17), we define $S(x) = \|x - \bar{x}_c\|^2$. Let $H(\tilde{x}, \bar{x}_c)$ be a hyperplane that is tangent to the sphere \mathcal{S} at point $x = \tilde{x}$ and cross the origin. The gradient of $S(x)$ at \tilde{x} is derived as $\nabla S(\tilde{x}) = 2(\tilde{x} - \bar{x}_c)^\top$. Since the tangent plane $H(\tilde{x}, \bar{x}_c)$ is orthogonal to $\nabla S(\tilde{x})$ at $x = \tilde{x}$, $H(\tilde{x}, \bar{x}_c)$ is described by the equation

$$\nabla S(\tilde{x}) \cdot (x - \tilde{x}) = 0. \quad (20)$$

Since the origin belongs to $H(\tilde{x}, \bar{x}_c)$, substituting $x = 0$ and $\nabla S(\tilde{x})$ into (20) gives

$$\|\tilde{x}\|^2 = \tilde{x}^\top \bar{x}_c. \quad (21)$$

When $n > 2$, there are infinitely many tangent planes $H(\tilde{x}, \bar{x}_c)$ of the sphere \mathcal{S} . The contacting points \tilde{x} are thus infinite, but all satisfy (21). Hence, the set of contacting points is characterized by the state set

$$\mathcal{X}_t = \{x \in \mathcal{R}_3 \mid \|x\|^2 = x^\top \bar{x}_c\}. \quad (22)$$

It follows from (22) that the contacting points x satisfy both $\|x - \bar{x}_c\|^2 = \bar{r}$ and $\|x\|^2 = x^\top \bar{x}_c$. Solving these two equations with \bar{x}_c and \bar{r} defined in (17) gives

$$\|x\|^2 = \phi(x_c) = (\eta_1\|x_c\|^2 - \eta_2)/(\eta_1 + 1). \quad (23)$$

Let $\hat{\mathcal{R}}_3 = \{x \in \mathcal{R}_3 \mid \|x\|^2 < \phi(x_c)\}$. Let $\mathcal{R}_{2,s}$ be the set of states enclosed by the hyperplanes and underneath

\mathcal{R}_3 , which satisfies $\mathcal{R}_{2,s} \subset \mathcal{R}_2$. An intuitive graphic view of these state sets are shown in Figure 2 for the simple 2-D example. When $x \in \hat{\mathcal{R}}_3$, the hyperplane H and the state set $\mathcal{R}_{2,s}$ all belong to the state region \mathcal{R}_2 where $V(x) = L(x) = \|x\|^2$. If the decreasing condition in \mathcal{R}_2 is satisfied, i.e. $L(x) = \|x\|^2$ converges (exponentially) to the origin, the level values of the hyperplane H are monotonically decreasing towards the origin. Hence, for all $x \in H \cap \hat{\mathcal{R}}_3$, the state trajectories will naturally converge to the origin, at least through the hyperplane H . This means that for any $x(0) \in \mathcal{X} \setminus (\mathcal{O} \cup \mathcal{R}_1 \cup \mathcal{R}_3)$, the state trajectory will never reach $\hat{\mathcal{R}}_3$ from below. Moreover, if the decreasing condition holds for the entire region \mathcal{R}_1 and the shrunk region $\mathcal{R}_3 \setminus \hat{\mathcal{R}}_3$, once the state trajectories reach $\mathcal{R}_3 \setminus \hat{\mathcal{R}}_3$ or enter \mathcal{R}_1 , they will be bounced back and eventually back to the region \mathcal{R}_2 . This means that the state trajectories starting from any $x(0) \in \mathcal{X} \setminus (\mathcal{O} \cup \mathcal{R}_1 \cup \mathcal{R}_3)$ do not reach $\hat{\mathcal{R}}_3$ from the above.

In summary, evaluation of the decreasing condition in \mathcal{R}_3 only needs to be performed for those states satisfying $\|x\|^2 \geq \phi(x_c)$. This concludes that the state region \mathcal{R}_3 in Theorem 3.4 can be shrunk by removing the state set $\hat{\mathcal{R}}_3$. It also implies that even in the special case that the state trajectory moves along \mathcal{R}_3 and close to the origin, it will leave \mathcal{R}_3 from the contacting points characterized by $\mathcal{X}_t = \{x \in \mathcal{R}_3 \mid \|x\|^2 = x^\top \bar{x}_c\}$ and converge to the origin. This confirms that \mathcal{R}_3 is not a limit cycle \square

As shown in the proof of Proposition 3.1, if starting from any $x(0) \in \mathcal{X} \setminus (\mathcal{O} \cup \mathcal{R}_1 \cup \mathcal{R}_3)$, the state trajectory does not reach the region $\hat{\mathcal{R}}_3$. Hence, $\hat{\mathcal{R}}_3$ can be ignored when evaluating the decreasing condition (14) for autonomous systems. The conclusion that \mathcal{R}_3 is not a limit cycle will be explicitly used when designing the controller for the non-autonomous system (1) in Section 4.

4 GenLBF-based control design

This section presents a systematic design of a piecewise state-feedback controller to ensure \mathcal{KL} -stability and safety of the system (1), based on the GenLBF constructed in Section 3.2. According to the upper generalized derivatives obtained in (15), an effective control needs to ensure satisfaction of the condition (2c) in all the three state regions \mathcal{R}_i , $i \in [1, 3]$, specified in (16).

4.1 Controller design

For the non-autonomous system (1) and the GenLBF constructed in Section 3.2, the upper generalized derivative $\overline{M}_{\mathcal{F}}V(x)$ is directly obtained by replacing $F(x)$ in (15) with $f(x) + g(x)u$. According to the proof of Theorem 3.4, at the time step t , the upper generalized deriva-

tive of the state set \mathcal{R}_3 can also be represented as

$$\begin{aligned} \overline{M}_{\mathcal{F}}V(x(t)) &= 0.5(d_1(x(t)) + d_2(x(t))) \\ &\quad + \partial h_1 \cdot (d_1(x(t)) - d_2(x(t))), \\ \partial h_1 &= \begin{cases} -0.5, & h_2(x(t)) \rightarrow 0^- \\ 0.5, & h_2(x(t)) \rightarrow 0^+ \end{cases}, \end{aligned} \quad (24)$$

where $d_1(x) = P(x)(f(x) + g(x)u)$, $d_2(x) = 2x^\top(f(x) + g(x)u)$, $P(x) = -2\eta_1(x - x_c)^\top$, and $h_2(x(t)) = B(x(t)) - L(x(t))$.

Let $x(t - t_s)$ be the state value at one time step t_s backward. Then $\partial h_1 = 0.5\text{sign}(h_2(x(t - t_s)))$, where $\text{sign}(\cdot)$ is the signum function. Then it follows from (24) that

$$\begin{aligned} \overline{M}_{\mathcal{F}}V(x(t)) &= 0.5[1 + \text{sign}(h_2(x(t - t_s)))]d_1(x(t)) \\ &\quad + 0.5[1 - \text{sign}(h_2(x(t - t_s)))]d_2(x(t)). \end{aligned} \quad (25)$$

If $h_2(x(t - t_s)) < 0$, i.e. $x(t - t_s) \in \mathcal{R}_2$, then $h_2(x(t)) \rightarrow 0^-$ and $\text{sign}(h_2(x(t - t_s))) = -1$, i.e. the state trajectory approaches \mathcal{R}_3 from \mathcal{R}_2 at time t . If $h_2(x(t - t_s)) > 0$, i.e. $x(t - t_s) \in \mathcal{R}_1$, then $\text{sign}(h_2(x(t - t_s))) = 1$ and $h_2(x(t)) \rightarrow 0^+$, i.e. the state trajectory approaches \mathcal{R}_3 from \mathcal{R}_1 at time t . Therefore, (25) is equivalent to

$$\overline{M}_{\mathcal{F}}V(x(t)) = \begin{cases} d_2(x(t)), & (x(t) \in \mathcal{R}_3) \cap (x(t - t_s) \in \mathcal{R}_2) \\ d_1(x(t)), & (x(t) \in \mathcal{R}_3) \cap (x(t - t_s) \in \mathcal{R}_1) \end{cases}. \quad (26)$$

The proposed control design requires an extra condition on $g(x)$ and η_1 as in Assumption 4.1.

Assumption 4.1 *System (1) satisfies the following conditions:*

$$\begin{aligned} 2x^\top f(x) &\leq 0, \quad \forall x \in \{x \in \mathcal{R}_2 \setminus \{0\} \mid 2x^\top g(x) = 0\}, \\ P(x)f(x) &< 0, \quad \forall x \in \{x \in \mathcal{R}_1 \cup \mathcal{R}_3 \mid P(x)g(x) = 0\}, \end{aligned}$$

where $P(x) = -2\eta_1(x - x_c)^\top$. Moreover, the system is zero-state detectable with respect to $2x^\top g(x)$ and $P(x)g(x)$, i.e., $\forall t \geq 0$,

$$2x^\top g(x) = 0 \implies x(t) \rightarrow 0; \quad P(x)g(x) = 0 \implies x(t) \rightarrow 0.$$

By defining the generalized derivative of the GenLBF $V(x)$ along $f(x)$ and $g(x)$ as $G_fV(x)$ and $G_gV(x)$, respectively, Assumption 4.1 is compactly expressed as

$$\begin{aligned} G_fV(x) &\leq 0 \quad \forall x \in \{x \in \mathcal{X} \setminus \{0\} \mid G_gV(x) = 0\}, \\ G_gV(x) &= 0 \quad \forall t \geq 0 \implies x(t) \rightarrow 0. \end{aligned}$$

In this sense, Assumption 4.1 is the requirement of properness of the GenLBF, which is also necessary for the CLBF-based control design (Romdlony & Jayawardhana, 2016). The proposed GenLBF-based control design is described in Theorem 4.1.

Theorem 4.1 Consider system (1) under Assumptions 2.1 and 4.1, with the state space \mathcal{X} and a given unsafe state set \mathcal{O} in (11). By constructing the GenLBF $V(x)$ as in (12), this system is \mathcal{KL} -stable and safe for all $x(0) \in \mathcal{X} \setminus (\mathcal{O} \cup \mathcal{R}_1)$ under the following controller:

$$u = \kappa_i, x \in \mathcal{R}_i, i \in [1, 3] \quad (27)$$

with $\mathcal{R}_i, i \in [1, 3]$, in (16) and the three feedback laws

$$\kappa_1(x) = \begin{cases} -\mu(B_g)B_f - \mathbf{c}_1\bar{\mu}(B_g)\|x\|^2, & B_g \neq 0 \\ 0, & B_g = 0 \end{cases}, \quad (28a)$$

$$\kappa_2(x) = \begin{cases} -(L_f + \sqrt{L_f^2 + \gamma\|L_g\|^4})\mu(L_g), & L_g \neq 0 \\ 0, & L_g = 0 \end{cases}, \quad (28b)$$

$$\kappa_3(x) = \begin{cases} \kappa_1(x), & (x(t) \in \mathcal{R}_3) \cap (x(t-t_s) \in \mathcal{R}_1) \\ \kappa_2(x), & (x(t) \in \mathcal{R}_3) \cap (x(t-t_s) \in \mathcal{R}_2) \\ \kappa_2(x), & (x(t) \in \mathcal{R}_3) \cap (x(t-t_s) \in \mathcal{R}_3) \end{cases}, \quad (28c)$$

where $B_f := \frac{\partial B(x)}{\partial x}f(x) = P(x)f(x)$, $B_g := \frac{\partial B(x)}{\partial x}g(x) = P(x)g(x)$, $P(x) = -2\eta_1(x - x_c)^\top$, $L_f := \frac{\partial L(x)}{\partial x}f(x) = 2x^\top f(x)$ and $L_g := \frac{\partial L(x)}{\partial x}g(x) = 2x^\top g(x)$. The design constants $\mathbf{c}_1 = \text{diag}(c_{1,1}, \dots, c_{1,m}) > 0$ and $\gamma > 0$, while η_1 and η_2 satisfy (13).

Proof. Following the proof of Theorem 3.4, the GenLBF $V(x)$ in (12) satisfies conditions (2a) - (2b) trivially, because they are independent of u . Hence, we only need to show that the controller (27) ensures satisfaction of (2c). The upper generalized derivative of $V(x)$ can be derived as in (15) by replacing $F(x) = f(x) + g(x)u$. We show that (27) ensures satisfaction of (2c) in all the three regions $\mathcal{R}_i, i \in [1, 3]$.

1) *Region \mathcal{R}_1 :* In this region, $V(x) = B(x)$. Let $B_f := \frac{\partial B(x)}{\partial x}f(x) = P(x)f(x)$, $B_g := \frac{\partial B(x)}{\partial x}g(x) = P(x)g(x)$ and $P(x) = -2\eta_1(x - x_c)^\top$. Under the controller $u = \kappa_1(x)$ in (28a), the corresponding upper generalized derivative $\bar{M}_{\mathcal{F}}V(x) = P(x)(f(x) + g(x)\kappa_1(x)) = B_f + B_g\kappa_1(x)$. Note that $B_g\mu(B_g)B_f = B_f$ and $B_g\mathbf{c}_1\bar{\mu}(B_g)\|x\|^2 = \bar{c}_1\|x\|^2$, where $\bar{c}_1 = \sum_{j=1}^n c_{1,j} > 0$. Hence, $\bar{M}_{\mathcal{F}}V(x)$ becomes

$$\bar{M}_{\mathcal{F}}V(x) = \begin{cases} -\bar{c}_1\|x\|^2, & B_g \neq 0 \\ B_f, & B_g = 0 \end{cases}. \quad (29)$$

According to Assumption 4.1, $B_f < 0$ when $B_g = 0$. Hence, it follows from (29) that there exists a \mathcal{P} -class function $\rho(\|x\|) = \rho_0\|x\|^2$ with a constant $\rho_0 > 0$ such that $\forall x \in \mathcal{R}_1, \bar{M}_{\mathcal{F}}V(x) \leq -\rho(\|x\|)$. Therefore, the condition (2c) is satisfied.

2) *Region \mathcal{R}_2 :* In this case, the GenLBF $V(x)$ reverts to be the CLF, i.e. $V(x) = L(x) = \|x\|^2$. Let

$L_f := \frac{\partial L(x)}{\partial x}f(x) = 2x^\top f(x)$ and $L_g := \frac{\partial L(x)}{\partial x}g(x) = 2x^\top g(x)$. The controller $u = \kappa_2(x)$ is designed in the form of Sontag's universal control law as in (28b). Since $2x^\top(f(x) + g(x)\kappa_2(x)) = L_f + L_g\kappa_2(x)$, under the controller $u = \kappa_2(x)$ in (28b), the corresponding upper generalized derivative $\bar{M}_{\mathcal{F}}V(x)$ becomes

$$\bar{M}_{\mathcal{F}}V(x) = \begin{cases} -\sqrt{L_f^2 + \gamma\|L_g\|^4}, & L_g \neq 0 \\ L_f, & L_g = 0 \end{cases}. \quad (30)$$

According to Assumption 4.1, $L_f < 0$ when $L_g = 0$. Hence, it follows from (30) that there exists a \mathcal{P} -class function $\rho(\|x\|) = \rho_0\|x\|^2$ with a constant $\rho_0 > 0$ such that $\forall x \in \mathcal{R}_2 \setminus \{0\}, \bar{M}_{\mathcal{F}}V(x) \leq -\rho(\|x\|)$. This means that the condition (2c) is satisfied.

3) *Region \mathcal{R}_3 :* The design of $u(t) = \kappa_3(x(t))$ in (28c) is divided into three disjoint cases based on the location of the previous time step state $x(t-t_s)$.

When $(x(t) \in \mathcal{R}_3) \cap (x(t-t_s) \in \mathcal{R}_1)$, it follows from (26) that the corresponding upper generalized derivative $\bar{M}_{\mathcal{F}}V(x) = d_1(x) = P(x)(f(x) + g(x)u)$. According to the proof of Region \mathcal{R}_1 , designing $\kappa_3(x) = \kappa_1(x)$ directly leads to satisfaction of the condition (2c).

When $(x(t) \in \mathcal{R}_3) \cap (x(t-t_s) \in \mathcal{R}_2)$, it follows from (26) that the corresponding upper generalized derivative $\bar{M}_{\mathcal{F}}V(x) = d_2(x) = 2x^\top(f(x) + g(x)u)$. According to the proof of Region \mathcal{R}_2 , designing $\kappa_3(x) = \kappa_2(x)$ directly leads to satisfaction of the condition (2c).

For completion, we further consider the case when $(x(t) \in \mathcal{R}_3) \cap (x(t-t_s) \in \mathcal{R}_3)$. In such case, the state trajectory is moving along \mathcal{R}_3 at time t . By designing $\kappa_3(x(t)) = \kappa_2(x(t))$, it ensures that the state trajectory has a gradient tangent to \mathcal{R}_3 and pointing to the origin. Hence, the state trajectory will keep moving along \mathcal{R}_3 towards the origin. According to Proposition 3.1, when the state trajectory arrives at the set of contacting points characterized by $\mathcal{X}_t = \{x \in \mathcal{R}_3 \mid \|x\|^2 = x^\top \bar{x}_c\}$, it will leave \mathcal{R}_3 and converge to the origin.

Summing up, the proposed piecewise controller (27) ensures satisfaction of (2c). It follows from Theorem 3.1 that under the proposed controller, system (1) is \mathcal{KL} -stable w.r.t. 0 and its trajectory never enters \mathcal{O} . \square

When the system (1) is fully-actuated, we have $n = m$ and $g(x)$ has full rank n . Then κ_1 can be replaced by $\kappa_1(x) = -g(x)^{-1}[\mu(P(x))P(x)f(x) + \mathbf{c}_1\bar{\mu}(P(x))\|x\|^2]$. The proposed controller involves designing the constants $c_{1,i}, i \in [1, m], \gamma, \eta_1$ and η_2 . The way to select them is described as follows:

- $c_{1,i}, i \in [1, m]$, and γ can be any positive constants. In general, bigger values of $c_{1,i}, i \in [1, m]$, and γ results

in bigger control actions and can make the state trajectories converge to the desired equilibrium faster.

- η_1 can be any constant satisfying (13) and η_2 is determined by using η_1 and choosing w . The choice of η_1 and w directly affects the buffer width $b_w = \sqrt{w/(\eta_1 + 1)}$. Increasing the buffer size improves state safety but reduces the allowable initial state space. Hence, their choice may need to take into account of the specific practical system preference.

As shown in Braun & Kellett (2017); Braun et al. (2019), applying merely the continuous universal control law constructed from the smooth CLBF (Romdlony & Jayawardhana, 2016) can prevent the state entering the unsafe region, but may steer the state into undesired local equilibriums. This happens at the points where gradients of CLF and CBF cancel each other, even for simple second-order linear systems as demonstrated in Braun & Kellett (2017). In this paper, by constructing the GenLBF with the form of (12), the issue of gradient cancellation is eliminated, making the control design more effective than the CLBF-based control law. Performance comparison of the proposed method and CLBF-based method will be demonstrated by simulation examples in Section 6.

4.2 Enhancing performance via control refinement

It should be noted that when the system has particular structures and the initial states fall into some set, then the state trajectories cannot be steered to the desired equilibrium $x_g = 0$ by the proposed controller (27). We illustrate this issue using Example 4.2, where the two state variables are controlled independently.

Example 4.2 Consider the mobile robot navigation system (Romdlony & Jayawardhana, 2016, Example 6.2):

$$\dot{x}_1 = u_1, \quad \dot{x}_2 = u_2, \quad (31)$$

which can be rewritten in the form of (1) with $x = [x_1, x_2]^\top$, $u = [u_1, u_2]^\top$, $f(x) = 0$ and $g(x) = I_2$. The operating state space is $\mathcal{X} := [-5, 5] \times [-5, 5]$. The control goal is to steer x to the origin $(0, 0)$ whilst avoiding the unsafe states in $\mathcal{D} := (1, 3) \times (-1, 1)$. The unsafe states can be enclosed by the unsafe set $\mathcal{O} = \{x \in \mathcal{X} \setminus \{0\} \mid \|x - x_c\| < \sqrt{2}\}$ with the centre $x_c = [2, 0]^\top$.

For this example system, $B_f = P(x)f(x) = 0$, $L_f = 2x^\top f(x) = 0$, $B_g = P(x)g(x) \neq 0$ for all $x \in \mathcal{X} \setminus \mathcal{O}$ and $Lg = 2x^\top g(x) \neq 0$ for all $x \in \mathcal{X} \setminus (\mathcal{O} \cup \{0\})$. According to Theorem 4.1, for all $x \in \mathcal{X} \setminus (\mathcal{O} \cup \{0\})$, $\kappa_1(x)$ and $\kappa_2(x)$ are designed as

$$\kappa_1(x) = 2\eta_1 \|x\|^2 \begin{bmatrix} \frac{c_{1,1}(x_1-2)}{(x_1-2)^2} \\ \frac{c_{1,2}x_2}{x_2^2} \end{bmatrix}, \quad \kappa_2(x) = -2\sqrt{\gamma} \begin{bmatrix} x_1 \\ x_2 \end{bmatrix}. \quad (32)$$

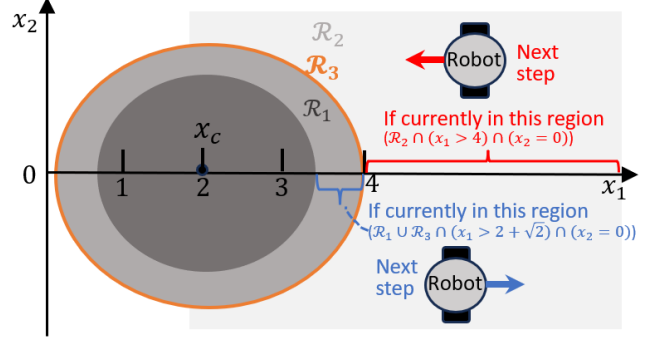


Fig. 3. Illustration of the robot's moving back and forth near the boundary \mathcal{R}_3 if $x(0)$ is on the right-hand side of the x_1 -axis with $x_1(0) > 4$. The robot's moving direction is indicated by the arrows, where it towards left in the region \mathcal{R}_2 and towards right in the regions \mathcal{R}_1 and \mathcal{R}_3 .

Suppose that the robot's initial position $x(0)$ is on the right-hand side of the x_1 -axis with $x_1(0) > 4$ and $x_2(0) = 0$. Since $x(0) \in \mathcal{R}_2$, $u = \kappa_2(x)$ is activated and $u_1(0) = -2\sqrt{\gamma}x_1(0) < 0$ and $u_2(0) = 0$. The robot moves on the x_1 -axis from right to left (towards the origin). For $t \geq 0$, $u_1(t) = -2\sqrt{\gamma}x_1(t) < 0$ and $u_2(t) = 0$, and the robot continues moving towards the origin on the x_1 -axis until reaches \mathcal{R}_3 . When arriving at \mathcal{R}_3 , $x_1(t) > 3$ and $x_2(t) = 0$. Since $(x(t) \in \mathcal{R}_3) \cap (x(t - t_s) \in \mathcal{R}_2)$, $u = \kappa_2(x)$ is used and the robot continues to move on the x_1 -axis and enter \mathcal{R}_1 . When the robot is in \mathcal{R}_1 , $x_1(t) > 3$, $x_2(t) = 0$ and $u = \kappa_1(x)$ is activated. According to (32), in this case $u_1(t) > 0$ and $u_2(t) = 0$. Hence, the robot will keep moving on the x_1 -axis, but now from left to right. When the robot arrives at \mathcal{R}_3 with $(x(t) \in \mathcal{R}_3) \cap (x(t - t_s) \in \mathcal{R}_1)$, it will keep using $u = \kappa_1(x)$ and move on the x_1 -axis from left to right. Once the robot moves back into the region \mathcal{R}_2 , $u = \kappa_2(x)$ is activated, and it again moves towards left. Finally, the robot will keep moving back and forth on the x_1 -axis near \mathcal{R}_3 . In summary, if the robot starts from the right-hand side of the x_1 -axis with $x_1(0) > 4$ and $x_2(0) = 0$, it will be stuck in the neighbourhood of \mathcal{R}_3 on the x_1 -axis and fail to reach the goal $(0, 0)$. This is graphically illustrated in Fig. 3.

Currently there are no systematic ways to determine the exact types of system structures that the controller (27) cannot handle. This section presents a generic, systematic strategy for refining the controller (27) to help the state trajectories escape from the undesired local points.

In the region \mathcal{R}_2 where $B(x) < L(x)$, the state trajectories are away from the unsafe region and the GenLBF becomes a standard CLF $V(x) = L(x) = \|x\|^2$. Hence, the universal control law $u = \kappa_2(x)$ ensures that the state trajectories converge to the desired equilibrium $x_g = 0$. In the proposed control design, the initial states are required to be in the region \mathcal{R}_2 , but they may enter the regions \mathcal{R}_1 or \mathcal{R}_3 due to physical reasons like inertia of a mobile robot. As shown in Proposition 3.1, \mathcal{R}_3 is not a limit cycle and the states slide on \mathcal{R}_3 will leave it at the

contacting points and converge to the origin. However, in the regions \mathcal{R}_1 , GenLBF is no longer the standard CLF and convergence to the desired equilibrium is not always guaranteed under the proposed control law. This motivates the proposal of refining the controller $u = \kappa_1(x)$ for the region \mathcal{R}_1 to escape the state trajectory from undesired local points.

Note that the controller $\kappa_1(x)$ is dependent on $P(x) = -2\eta_1(x - x_c)^\top$ and subsequently on the unsafe region centre x_c . Therefore, the proposed strategy for refining $\kappa_1(x)$ is described as follows:

1) At time t , a suspicious local equilibrium is detected if the following logic condition is true:

$$\mathcal{C} = (t > 0) \wedge (x(t) - x(t - t_s) \leq \Delta_x), \quad (33)$$

where the condition $x(t) - x(t - t_s) \leq \Delta_x$ is used to determine whether the state $x(t)$ is almost the same as the previous state $x(t - t_s)$ under the sampling time step t_s and threshold Δ_x . In this paper, we set $\Delta_x = 1.0e-5$.

2) When a suspicious local equilibrium is detected, we replace x_c by a virtual centre x_v given by

$$x_v = x_c + e, \quad (34)$$

where $e \in \mathbb{R}^n$ is a small perturbation to be designed. This perturbation deviates the control action from its original one and subsequently move the state away from this suspicious undesired equilibrium.

3) $\kappa_1(x)$ in (28) is refined as

$$\bar{\kappa}_1(x) = \begin{cases} -\mu(B_g)B_f - \mathbf{c}_1\bar{\mu}_e(B_g)\|x\|^2, & B_g \neq 0 \\ 0, & B_g = 0 \end{cases}, \quad (35)$$

where $\bar{\mu}_e(B_g) = \left[\frac{\bar{P}(x)g_1}{\|P(x)g_1\|}, \dots, \frac{\bar{P}(x)g_m}{\|P(x)g_m\|} \right]^\top$, $\bar{P}(x) = -2\eta_1(x - x_v)^\top$, and $g_i(x)$, $i \in [1, m]$, is the i -th column of $g(x)$.

Example 4.2 is revisited to provide an intuitive illustration of the control refinement. When the robot is in the region \mathcal{R}_1 , by applying the virtual centre x_v with $e = [e_1, e_2]^\top$, the controller $\kappa_1(x)$ becomes $\bar{\kappa}_1(x) = 2\eta_1\|x\|^2[c_{1,1}(x_1 - 2 - e_1)/(x_1 - 2)^2, c_{1,2}(x_2 - e_2)/x_2^2]^\top$. By designing e_1, e_2 such that $x_1 - 2 - e_1 > 0$ and $e_2 \neq 0$, then $u_1 > 0$ and $u_2 \neq 0$. This enables the robot to move away from the x_1 -axis, either upward if $e_2 > 0$ or downward if $e_2 < 0$, thus escaping from the local equilibrium. Theorem 4.3 shows that the decreasing condition (2c) remains satisfaction under switching between the controllers $u = \kappa_1(x)$ and $u = \bar{\kappa}_1(x)$.

Theorem 4.3 *When $x \in \mathcal{R}_1$, the decreasing condition (2c) is satisfied by implementing the following controller:*

$$u = \begin{cases} \bar{\kappa}_1(x), & \mathcal{C} \text{ in (33) is true} \\ \kappa_1(x), & \text{otherwise} \end{cases}, \quad (36)$$

where e is chosen such that for all $i \in [1, m]$,

$$(x - x_c)^\top g_i(x)g_i(x)^\top e < \|(x - x_c)^\top g_i(x)\|^2. \quad (37)$$

Proof. By design, when the logic condition \mathcal{C} in (33) is true, the refined controller $u = \bar{\kappa}_1(x)$ in (35) is activated. By applying the refined controller, the upper generalized derivative in the region \mathcal{R}_1 with $B_g \neq 0$ becomes

$$\bar{M}_{\mathcal{F}}V(x) = -B_g\mathbf{c}_1\bar{\mu}_e(B_g)\|x\|^2. \quad (38)$$

Since $P(x) = -2\eta_1(x - x_c)^\top$, $\bar{P}(x) = -2\eta_1(x - \bar{x}_c)^\top$ and $\bar{x}_c = x_c + e$, the inequality (37) implies $P(x)g_i(x)(\bar{P}(x)g_i(x))^\top > 0$ and subsequently $P(x)g_i(x)\mathbf{c}_{1,i}(\bar{P}(x)g_i(x))^\top > 0$. It then follows that $B_g\mathbf{c}_1\bar{\mu}_e(B_g) > 0$. Submitting this to (38) yields

$$\bar{M}_{\mathcal{F}}V(x) = -\bar{c}_1\|x\|^2, \quad (39)$$

where $\bar{c}_1 = B_g\mathbf{c}_1\bar{\mu}_e(B_g)$.

The case when $B_g = 0$ remains the same as that in Theorem 4.1. Hence, there exists a \mathcal{P} -class function $\rho(\|x\|) = \rho_0\|x\|^2$ with a constant $\rho_0 > 0$ such that $\forall x \in \mathcal{R}_1$,

$$\bar{M}_{\mathcal{F}}V(x) = P(x)(f(x) + g(x)\bar{\kappa}_1(x)) \leq -\rho(\|x\|). \quad (40)$$

Therefore, the condition (2c) is satisfied.

When the logic condition \mathcal{C} is false, $u = \kappa_1(x)$ is activated. As shown in Section 4.1, this controller always ensures satisfaction of (2c) in the region \mathcal{R}_1 . To complete the proof, it is worth noting that when the state arrives at $x = 0$, $u = \kappa_1(0) = \bar{\kappa}_1(0) = 0$. Hence, the state will remain at the desired equilibrium 0. \square

Theorem 4.3 shows that by designing the perturbation e to fulfil the specified requirements, the proposed control refinement will not affect safe stabilization of the system. Given the known nonlinear function $g(x)$ and unsafe state set parameters x_c , a suitable e can be found by solving the nonlinear optimization problem:

$$\min_{e,x} \|e\|^2 \quad (41)$$

$$\text{s.t. (37), } e \in [\underline{e}, \bar{e}], e(j)^2 > 0, j \in [1, n], x \in \mathcal{R}_1,$$

where $[\underline{e}, \bar{e}]$, with $\underline{e} < 0$ and $\bar{e} > 0$, is a pre-defined searching interval for improving the solution efficiency. This nonlinear optimization problem only needs to be

solved once before implementing the control law using off-the-self solvers such as the Matlab *fmincon*. Therefore, computational burden is not a concern.

5 Handling multiple unsafe state sets

Sections 3 and 4 present the methods for constructing a GenLBF and the corresponding piecewise feedback control law for the system (1) with a single unsafe state set. In this section, we will show that these methods are directly extended to handle multiple unsafe state sets.

We consider that there are N disjoint unsafe state sets in the state space \mathcal{X} , where the i -th unsafe set is enclosed by an open ball \mathcal{O}_i defined as

$$\mathcal{O}_i = \{x \in \mathcal{X} \setminus \{0\} \mid \|x - x_{i,c}\| < \sqrt{r_i}\}, \quad (42)$$

where $x_{i,c}$ is the centre and $\sqrt{r_i}$ is the radius. The enclosure of \mathcal{O}_i is denoted as $\bar{\mathcal{O}}_i$.

Theorem 5.1 provides a way for constructing a single GenLBF to certify \mathcal{KL} -stability and safety of an autonomous system in the presence of N unsafe state sets.

Theorem 5.1 *Consider the system $\dot{x} = F(x)$ under Assumption 2.1 with the state space \mathcal{X} and the unsafe state sets $\mathcal{O}_i, i \in [1, N]$, in (42). This system is \mathcal{KL} -stable and safe for all $x(0) \in \mathcal{X} \setminus (\mathcal{O} \cup (\cup_{i=1}^N \mathcal{R}_{i,1}) \cup (\cup_{i=1}^N \mathcal{R}_{i,3}))$, where $\mathcal{O} = \cup_{i=1}^N \mathcal{O}_i$, if*

1) The GenLBF $V(x)$ is constructed as

$$V(x) = \max(L(x), \max_{i \in [1, N]} B_i(x)), L(x) = \|x\|^2, \\ B_i(x) = \eta_{i,2} - \eta_{i,1} \|x - x_{i,c}\|^2, i \in [1, N] \quad (43)$$

with the design constants $\eta_{i,1}$ and $\eta_{i,2}$ satisfying

$$\eta_{i,1} > (\|x_{i,c}\| + \sqrt{r_i}) / (\|x_{i,c}\| - \sqrt{r_i}), \quad (44a)$$

$$\eta_{i,2} = \eta_{i,1} r_i + \max_{x \in \bar{\mathcal{O}}_i} \|x\|^2 + w_i, \quad (44b)$$

$$\|x_{i,c} - x_{j,c}\| > \sqrt{r_i} + \sqrt{r_j}, \forall i, j \in [1, N], i \neq j, \quad (44c)$$

where $0 < w_i < \eta_{i,1} (\|x_{i,c}\|^2 - r_i) - (\|x_{i,c}\| + \sqrt{r_i})^2$ and $\bar{r}_i = \frac{(1+\eta_{i,1})\eta_{i,2} - \eta_{i,1}\|x_{i,c}\|^2}{(1+\eta_{i,1})^2}$, $i \in [1, N]$.

2) There exists a function $\rho(\|x\|) \in \mathcal{P}$ satisfies

$$\bar{M}_{\mathcal{F}} V(x) \leq -\rho(\|x\|) \quad (45)$$

with $\bar{M}_{\mathcal{F}} V(x)$ in the form of

$$\bar{M}_{\mathcal{F}} V(x) = \begin{cases} d_{i,1}(x), & x \in \mathcal{R}_{i,1}, i \in [1, N] \\ d_2(x), & x \in \mathcal{R}_2 \\ d_{i,3}(x), & x \in \mathcal{R}_{i,3} \setminus \hat{\mathcal{R}}_{i,3}, i \in [1, N] \end{cases}$$

where $d_{i,1}(x) = P_i(x)F(x)$, $d_2(x) = 2x^\top F(x)$, $d_{i,3} = 0.5(d_{i,1}(x) + d_2(x)) + 0.5|d_{i,1}(x) - d_2(x)|$, $P_i(x) = -2\eta_{i,1}(x - x_{i,c})^\top$, and

$$\begin{aligned} \mathcal{R}_{i,1} &= \{x \in \mathcal{X} \mid x \notin \mathcal{O}, \\ &\quad B_i(x) > \max(L(x), \{B_j(x)\}_{j=1, j \neq i}^N)\}, \\ \mathcal{R}_2 &= \{x \in \mathcal{X} \mid \max_{j \in [1, N]} B_j(x) < L(x)\}, \\ \mathcal{R}_{i,3} &= \{x \in \mathcal{X} \mid B_i(x) = L(x)\}, \\ \hat{\mathcal{R}}_{i,3} &= \{x \in \mathcal{R}_{i,3} \mid \|x\|^2 < \phi(x_{i,c})\}, \end{aligned} \quad (46)$$

where $\phi(x_{i,c}) = (\eta_{i,1}\|x_{i,c}\|^2 - \eta_{i,2}) / (\eta_{i,1} + 1)$.

The proof of Theorem 5.1 follows directly from that of Theorem 3.4, despite that \mathcal{R}_1 and \mathcal{R}_3 become $\mathcal{R}_{i,1}$ and $\mathcal{R}_{i,3}$, $i \in [1, N]$, respectively. Nevertheless, the proof of each $\mathcal{R}_{i,1}$ and $\mathcal{R}_{i,3}$ is analogous, respectively. It is worth noting the design constants $\eta_{i,1}$ and $\eta_{i,2}$, $i \in [1, N]$, are required to satisfy an extra condition (44c). According to (17), for the proposed GenLBF (43), the points satisfying $x \in \mathcal{R}_{i,3}$ can be described as a sphere:

$$\|x - \bar{x}_{c,i}\|^2 = \bar{r}_i \quad (47)$$

with the centre $\bar{x}_{c,i} = \frac{\eta_{i,1}}{1+\eta_{i,1}} x_{i,c}$ and radius $\sqrt{\bar{r}_i}$ satisfying $\bar{r}_i = [(1+\eta_{i,1})\eta_{i,2} - \eta_{i,1}\|x_{i,c}\|^2] / (1+\eta_{i,1})^2$, $i \in [1, N]$. Hence, by imposing the extra requirement in (44c), the spheres for all unsafe sets are guaranteed to be disjoint.

Similar to Assumption 4.1, the proposed control design for multiple unsafe state sets requires Assumption 5.1.

Assumption 5.1 *For all $x \in \{x \in \mathcal{R}_2 \setminus \{0\} \mid 2x^\top g(x) = 0\}$, $2x^\top f(x) \leq 0$. For all $x \in \{x \in \mathcal{R}_{i,1} \cup \mathcal{R}_{i,3} \mid P_i(x)g(x) = 0\}$, $P_i(x)f(x) < 0$, where $P_i(x) = -2\eta_{i,1}(x - x_{i,c})^\top$, $i \in [1, N]$. Moreover, the system is zero-state detectable with respect to $2x^\top g(x)$ and $P_i(x)g(x)$, i.e., $2x^\top g(x) = 0 \forall t \geq 0 \implies x(t) \rightarrow 0$ and $P_i(x)g(x) = 0 \forall t \geq 0 \implies x(t) \rightarrow 0$, $i \in [1, N]$.*

The way of designing an effective controller to handle multiple unsafe regions is described in Theorem 5.2.

Theorem 5.2 *Consider system (1) under Assumptions 2.1 and 5.1, with the state space \mathcal{X} and disjoint unsafe state sets $\mathcal{O}_i, i \in [1, N]$, in (42). By constructing the GenLBF as in (43), this system is safe and \mathcal{KL} -stable for all $x(0) \in \mathcal{X} \setminus (\mathcal{O} \cup (\cup_{i=1}^N \mathcal{R}_{i,1}) \cup (\cup_{i=1}^N \mathcal{R}_{i,3}))$, where $\mathcal{O} = \cup_{i=1}^N \mathcal{O}_i$, if the controller is designed as*

$$u = \begin{cases} \kappa_{i,1}(x), & x \in \mathcal{R}_{i,1}, i \in [1, N] \\ \kappa_2(x), & x \in \mathcal{R}_2 \\ \kappa_{i,3}(x), & x \in \mathcal{R}_{i,3}, i \in [1, N] \end{cases} \quad (48)$$

with

$$\kappa_{i,1}(x) = \begin{cases} -\mu(B_{g,i})B_{f,i} - \mathbf{c}_{i,1}\bar{\mu}(B_{g,i})\|x\|^2, & B_{g,i} \neq 0 \\ 0, & B_{g,i} = 0 \end{cases},$$

$$\kappa_2(x) = \begin{cases} -(L_f + \sqrt{L_f^2 + \gamma\|L_g\|^4})\mu(L_g), & L_g \neq 0 \\ 0, & L_g = 0 \end{cases},$$

$$\kappa_{i,3}(x) = \begin{cases} \kappa_{i,1}(x), & (x(t) \in \mathcal{R}_{i,3}) \cap (x(t-t_s) \in \mathcal{R}_{i,1}) \\ \kappa_2(x), & (x(t) \in \mathcal{R}_{i,3}) \cap (x(t-t_s) \in \mathcal{R}_2) \\ \kappa_2(x), & (x(t) \in \mathcal{R}_{i,3}) \cap (x(t-t_s) \in \mathcal{R}_{i,3}) \end{cases},$$

where $B_{f,i} := \frac{\partial B_i(x)}{\partial x} f(x) = P_i(x)f(x)$, $B_{g,i} := \frac{\partial B_i(x)}{\partial x} g(x) = P_i(x)g(x)$, $P_i(x) = -2\eta_{i,1}(x - x_{i,c})^\top$, $L_f = 2x^\top f(x)$ and $L_g = 2x^\top g(x)$. The design constants $\mathbf{c}_{i,1} = \text{diag}(c_{i,1,1}, \dots, c_{i,1,j}) > 0$, $j \in [1, m]$, and $\gamma > 0$, while $\eta_{i,1}$ and $\eta_{i,2}$ satisfy (44). The state regions $\mathcal{R}_{i,1}$, \mathcal{R}_2 and $\mathcal{R}_{i,3}$, $i \in [1, N]$, are defined in (46).

The proof of Theorem 5.2 is trivial by using the proof of Theorem 4.1 and it is thus omitted here. The control refinement strategy described in Section 4.2 is directly applicable to the case of multiple unsafe state sets. Each control law $\kappa_{i,1}$, $i \in [1, N]$, is refined by adding the perturbation e_i solved from the optimization problem (41), whose detail is thus omitted here.

6 Illustrative examples

To demonstrate the efficacy of our proposed method comprehensively, we consider three simulation cases:

- *Case 1:* We utilize a linear numerical system with an unsafe state set to compare the performance of our non-refined control (refer to Section 4.1) and the CLBF-based control (Romdlony & Jayawardhana, 2016). Full details are in Section 6.1.
- *Case 2:* We utilize the mobile robot system in Example 4.2 with an unsafe state set to compare our non-refined control, refined control (refer to Section 4.2) and the CLBF-based control (Romdlony & Jayawardhana, 2016). Full details are in Section 6.2.
- *Case 3:* We utilize a nonlinear mechanical system with three unsafe state sets to demonstrate the effectiveness of our refined control. Full details are in Section 6.3.

6.1 Simulation Case 1

Consider the linear system (Braun & Kellett, 2017, Example 14) represented by

$$\dot{x}_1 = -x_1 + u_1, \quad \dot{x}_2 = -x_2 + u_2, \quad (49)$$

which can be rewritten in the form of (1) with $x = [x_1, x_2]^\top$, $u = [u_1, u_2]^\top$, $f(x) = -x$ and $g(x) = I_2$.

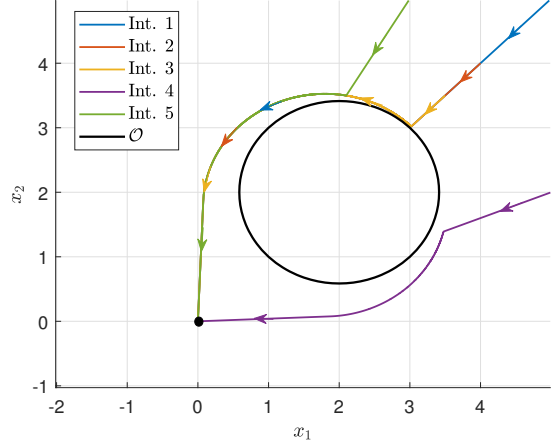


Fig. 4. State trajectories under five different initial (Int.) states: Case 1, our non-refined control.

The operating state space is $\mathcal{X} := [-5, 5] \times [-5, 5]$. The control goal is to steer x to the origin $(0, 0)$ while avoiding a set of unsafe states in $\mathcal{D} := (1, 3) \times (1, 3)$. The unsafe states in \mathcal{D} can be enclosed by the unsafe set $\mathcal{O} = \{x \in \mathcal{X} \setminus \{0\} \mid \|x - x_c\| < \sqrt{2}\}$, with the centre at $x_c = [2, 2]^\top$. Since $2x^\top g(x) = 2x^\top = 0$ only when $x = 0$ and $P(x)g(x) = -2\eta_1(x - x_c)^\top = 0$ only when $x = x_c$, Assumption 4.1 is satisfied automatically.

The design parameters of our method without the refinement are: $\eta_1 = 9$, $w = 0.9$, $\eta_2 = 36.9$, $\mathbf{c}_1 = \text{diag}(10, 20)$, $\gamma = 0.1$. A comparison is made with the CLBF method (Romdlony & Jayawardhana, 2016) by borrowing the design parameters from (Braun & Kellett, 2017, Example 14). Both controllers are simulated under five different initial (Int.) states $x(0)$: $(5, 5)$, $(4, 4)$, $(3.5, 3.5)$, $(5, 2)$, $(3, 5)$. It is seen from Figure 4 that the proposed controller steers the state to the origin while avoiding the unsafe set from all the five different initial conditions. However, as shown in Fig. 6, the CLBF-based controller is unable to steer the state trajectories to the origin when the initial states satisfy $x_1 = x_2 > 3$.

We further use the state trajectories and corresponding $V(x)$ values of Int. 1, Int. 4 and Int. 5 and three extra initial states, including Int. 6 $(0.2, 0.8)$, Int. 7 $(0.55, 0.55)$ and Int. 8 $(0.8, 0.2)$, in Fig. 5 to demonstrate soundness of the proposed idea of shrinking \mathcal{R}_3 in Proposition 3.1. According to Proposition 3.1, it is computed that $\phi(x_c) = 3.50$. Subsequently, the intersection points (i.e. contacting points of the tangent planes) of $\|x\|^2 = \phi(x_c)$ and \mathcal{R}_3 are computed as $\tilde{x} = (1.87, 0.08)$ and $\tilde{x} = (0.08, 1.87)$. As shown in Fig. 5, the contacting point $\tilde{x} = (1.87, 0.08)$ coincides with the actual point from which the state trajectory Int. 4 leaves \mathcal{R}_3 and converges straightly to the origin. Similarly, it is seen that the contacting point $\tilde{x} = (0.08, 1.87)$ coincides with the actual point from which the state trajectories Int. 1 and Int. 5

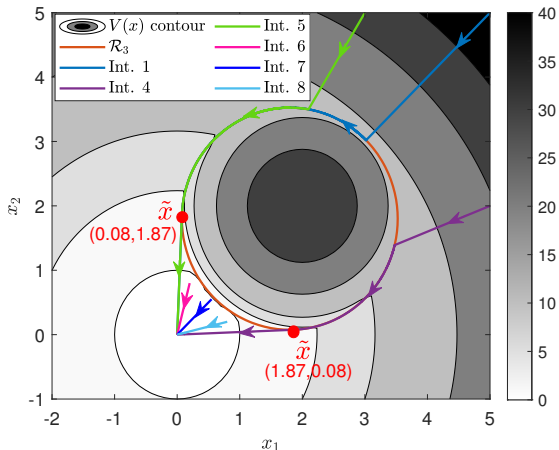


Fig. 5. State trajectories and corresponding $V(x)$ values of Int. 1, Int. 4, Int. 5, Int. 6, Int. 7 and Int. 8 used to demonstrate the idea of shrinking \mathcal{R}_3 in Proposition 3.1: Case 1, our non-refined control.

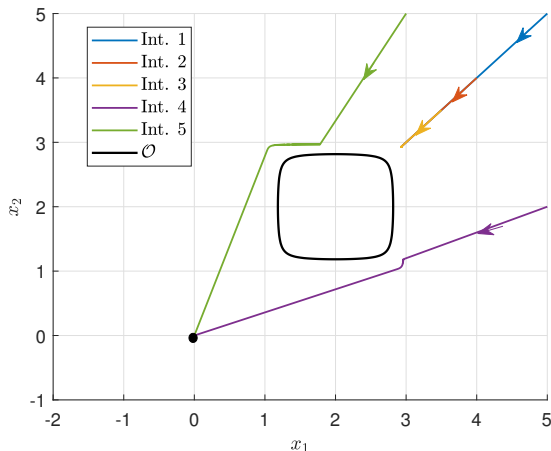


Fig. 6. State trajectories under five different initial (Int.) states: Case 1, CLBF method.

leave \mathcal{R}_3 and converge to the origin. The results in Fig. 5 thus confirm the claim that the state trajectories will not reach \mathcal{R}_3 from either above (Int. 1, Int. 4 and Int. 5) or below (Int. 6, Int. 7 and Int. 8), and they will converge to the origin. This shows soundness of Proposition 3.1.

6.2 Simulation Case 2

We consider the mobile robot navigation system as in Example 4.2 in Section 4.2 with the same state space $\mathcal{X} := [-5, 5] \times [-5, 5]$ and unsafe set $\mathcal{O} = \{x \in \mathcal{X} \setminus \{0\} \mid \|x - x_c\| < \sqrt{2}\}$ centred at $x_c = [2, 0]^\top$. Since $2x^\top g(x) = 2x^\top = 0$ only when $x = 0$ and $P(x)g(x) = -2\eta_1(x - x_c)^\top = 0$ only when $x = x_c$, Assumption 4.1 is satisfied automatically. The design parameters of our method without the refinement are: $\eta_1 = 8.5$, $w = 0.9$, $\eta_2 = 29.5$, $\mathbf{c}_1 = \text{diag}(10, 20)$, $\gamma = 10$. A comparison is made with the CLBF method (Romdlony & Jayaward-

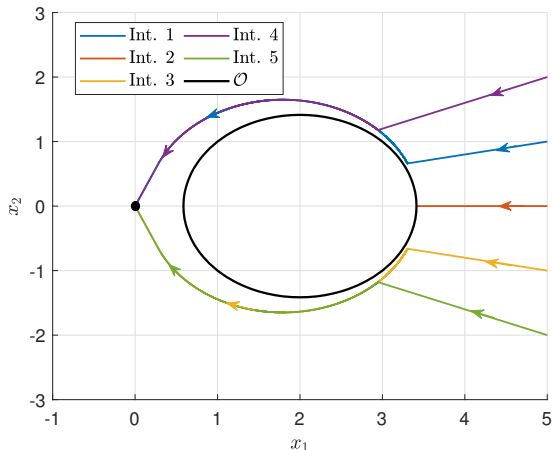


Fig. 7. State trajectories under five different initial (Int.) states: Case 2, our non-refined control.

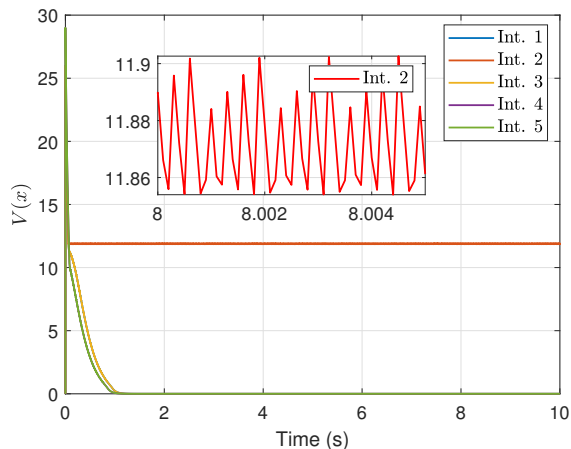


Fig. 8. Evolution of $V(x)$ under five different initial (Int.) states: Case 2, our non-refined control.

hana, 2016) by borrowing the design parameters from (Braun & Kellett, 2017, Example 15). Both controllers are simulated under five different initial (Int.) states $x(0)$: $(5, 1)$, $(5, 0)$, $(5, -1)$, $(5, 2)$, $(5, -2)$.

It is seen from Fig. 7 that the proposed controller steers the state to the origin while avoiding the unsafe set from all the initial conditions, except for Int. 2 $x(0) = (5, 0)$. This is also confirmed in Figure 8, where the GenLBF $V(x)$ has negative derivatives over time in all five different scenarios except for Int. 2 $x(0) = (5, 0)$. According to Example 4.2, the robot cannot be steered to the origin when it starts from any initial position $x(0)$ on the right-hand side of the x_1 -axis with $x_1(0) > 2 + \sqrt{2}$ and $x_2(0) = 0$. Figure 9 shows that the CLBF-based controller cannot steer the state to the origin when the initial state are near the x_1 -axis with $x_2 \in [-1, 1]$. This demonstrates that our non-refined control method is already more effective than the existing method.

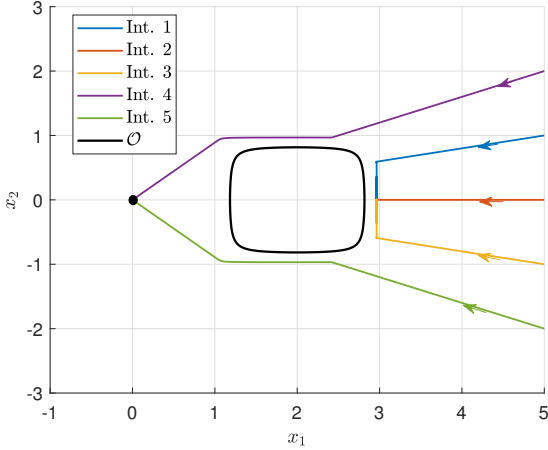


Fig. 9. State trajectories under five different initial (Int.) states: Case 2, CLBF method.

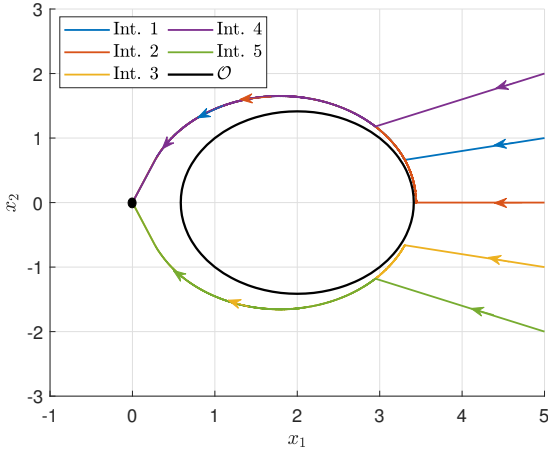


Fig. 10. State trajectories under five different initial (Int.) states: Case 2, our refined control.

We further refine our controller $\kappa_1(x)$ for the regions \mathcal{R}_1 and \mathcal{R}_3 with the perturbation $e = [3.2e-3, -3.2e-3]^\top$, which is solved from (41) using the Matlab nonlinear optimization solver *fmincon* with $\underline{e} = -1.0e-2$, $\bar{e} = 1.0e-2$, $e(1)^2 \geq 1.0e-5$, and $e(2)^2 \geq 1.0e-5$. As seen from Fig. 10, the refined controller ensures that the states converge to the origin safely under all initial conditions.

6.3 Simulation Case 3

Consider a nonlinear mechanical system modelled by

$$\dot{x}_1 = x_2, \quad \dot{x}_2 = -x_1 - x_2 + s(x) + u, \quad (50)$$

where $s(x) = -(0.8 + 0.2e^{-100|x_2|}) \tanh(10x_2)$. The state space is $\mathcal{X} := [-5, 5] \times [-5, 5]$ and there are three unsafe state sets $\mathcal{D}_1 := (1.2, 2.8) \times (-0.8, 0.8)$, $\mathcal{D}_2 := (1.3, 2.7) \times (1.3, 2.7)$, and $\mathcal{D}_3 := (-3, -1) \times (-1, 1)$. These unsafe state are enclosed by $\mathcal{O}_1 = \{x \in \mathcal{X} \setminus \{0\} \mid \|x - x_{1,c}\| <$

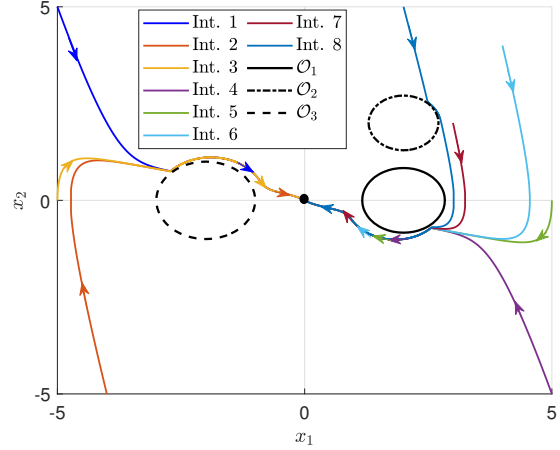


Fig. 11. State trajectories under eight different initial (Int.) states: Case 3, our refined method.

$\sqrt{0.7}\}$, $\mathcal{O}_2 = \{x \in \mathcal{X} \setminus \{0\} \mid \|x - x_{2,c}\| < \sqrt{0.5}\}$, and $\mathcal{O}_3 = \{x \in \mathcal{X} \setminus \{0\} \mid \|x - x_{3,c}\| < 1\}$ with $x_{1,c} = [2, 0]^\top$, $x_{2,c} = [2, 2]^\top$ and $x_{3,c} = [-2, 0]^\top$, respectively.

Since $2x^\top g(x) = 2x_2 = 0$ when $x_2 = 0$, $P_1(x)g(x) = -2\eta_{1,1}x_2 = 0$ when $x_2 = 0$, $P_2(x)g(x) = -2\eta_{2,1}(x_2 - 2) = 0$ when $x_2 = 2$, and $P_3(x)g(x) = -2\eta_{3,1}x_2 = 0$ when $x_2 = 0$. When $x_2 = 0$, $f(x) = [0, -x_1]^\top$ and thus $2x^\top f(x) = 0$, $P_1(x)f(x) = 0$ and $P_3(x)g(x) = 0$. When $x_2 = 2$, it is computed that $P_2(x)f(x) = -4\eta_{2,1}(x_2 - 2)x_1 = 0$. However, according to (50), $\dot{x}_1 = 0$ and $\dot{x}_2 = -x_1 + u$ when $x_2 = 0$. Hence, even with $u = 0$, the state trajectories x will always move away from the x_1 -axis (i.e. $x_2 = 0$) and converge to the desired equilibrium $x = 0$. In summary, Assumption 5.1 is satisfied.

For \mathcal{O}_1 , the design parameters are chosen as $\eta_{1,1} = 11$, $w_1 = 0.3$, $\eta_{1,2} = 16$, and $\mathbf{c}_{1,1} = 10$. For \mathcal{O}_2 , the design parameters are chosen as $\eta_{2,1} = 19$, $w_2 = 0.7$, $\eta_{2,2} = 22.7$, and $\mathbf{c}_{2,1} = 20$. For \mathcal{O}_3 , the design parameters are chosen as $\eta_{3,1} = 18$, $w_3 = 0.2$, $\eta_{3,2} = 27.2$, and $\mathbf{c}_{3,1} = 20$. The parameter γ is set as $\gamma = 5$. To refine the controller $\kappa_{i,1}$, $i \in [1, 3]$, we solve the optimization problem (41) with $-1.0e-3 \leq e_i \leq 1.0e-2$, $e_i(1)^2 \geq 1.0e-6$ and $e_i(2)^2 \geq 1.0e-5$, $i \in [1, 3]$, to obtain the perturbations $e_1 = e_2 = e_3 = [1.2e-3, 3.2e-3]^\top$.

Our refined controller is simulated under eight different initial (Int.) states $x(0) : (-5, 5), (-4, -5), (-5, 0), (5, -5), (5, 0), (4, 4), (3, 2), (2, 5)$. It is seen from Fig. 11 that the proposed controller steers the state trajectories to the origin while avoiding the unsafe sets for all eight different initial conditions.

7 Conclusions

This paper proposes the generalized (nonsmooth) Lyapunov barrier function (GenLBF) to solve the safe stabi-

lization problem for systems with multiple bounded unsafe sets. It addresses the fundamental issue encountered by the state-of-the-art methods for solving this problem, which are based on smooth Lyapunov barrier functions. The paper presents a systematic constructive design of GenLBFs along with a computational approach for deriving their generalized derivatives. Based on the constructed GenLBF, a piecewise continuous feedback control with a refinement strategy is designed to ensure safe stabilization. The effectiveness and advantages of the proposed approach are demonstrated through rigorous theoretical analysis and extensive numerical simulation studies. Future work will include: 1) extending the proposed approach to accommodate complex system operational requirements, including state constraints, by using Boolean logic operations to compose the requirements, and 2) developing a learning-based method for constructing GenLBFs for more general nonlinear systems whose dynamics may be unknown.

A Proof of Theorem 3.2

Proposition A.1 and Lemma A.1 will be used in the proof.

Proposition A.1 (Alefeld & Mayer, 2000) *Given the nonempty compact intervals on \mathbb{R} as $x = [\underline{x}, \bar{x}]$ and $y = [\underline{y}, \bar{y}]$, then the following rules hold:*

$$\begin{aligned} x + y &= [\underline{x} + \underline{y}, \bar{x} + \bar{y}], \\ x \cdot y &= [\min\{\underline{x}\underline{y}, \underline{x}\bar{y}, \bar{x}\underline{y}, \bar{x}\bar{y}\}, \max\{\underline{x}\underline{y}, \underline{x}\bar{y}, \bar{x}\underline{y}, \bar{x}\bar{y}\}]. \end{aligned}$$

Lemma A.1 (Cortes et al., 2024) *Let $\mathcal{F} : \mathbb{R}^n \times \mathbb{R}^m \mapsto \mathbb{R}^n$ be a set-valued map and take only nonempty, compact and convex values. Let the functions $h_1 : \mathbb{R} \mapsto \mathbb{R}$ and $h_2 : \mathbb{R}^n \mapsto \mathbb{R}^n$ be locally Lipschitz near x . Then $L_{\mathcal{F}}h_2(x, u) \cdot \partial h_1(h_2(x))$ is a nonempty compact interval.*

Proof. According to Clarke's first Chain Rule (Clarke, 1990, Theorem 2.3.9), the following relation holds:

$$\partial h(x) \subseteq \overline{\text{co}}\{\alpha\xi \mid \alpha \in \partial h_1(h_2(x)), \xi \in \partial h_2(x)\}, \quad (\text{A.1})$$

where $\overline{\text{co}}\{\cdot\}$ denotes the convex closure.

Define the set $\mathbb{W} := \{\langle v, \theta \rangle \in \mathbb{R} \mid v \in \mathcal{F}(x, u), \theta \in \text{co}\{\alpha\xi \mid \alpha \in \partial h_1(h_2(x)), \xi \in \partial h_2(x)\}\}$, where $\text{co}\{\cdot\}$ denotes the convex hull. Then following the proof of (Cortes et al., 2024, Theorem 1) yields

$$\mathbb{W} = \text{co}\{L_{\mathcal{F}}h_2(x, u) \cdot \partial h_1(h_2(x))\}. \quad (\text{A.2})$$

By applying Proposition A.1 and Lemma A.1, we take

the supremum of both sides of (A.2) and get

$$\begin{aligned} \sup \mathbb{W} &\leq \sup \{ \text{co}\{L_{\mathcal{F}}h_2(x, u) \cdot \partial h_1(h_2(x))\} \} \\ &= \sup \{ L_{\mathcal{F}}h_2(x, u) \cdot \partial h_1(h_2(x)) \} \\ &= \max \{ \underline{M}_{\mathcal{F}}h_2(x, u) \cdot \underline{\partial}h_1(h_2(x)), \\ &\quad \underline{M}_{\mathcal{F}}h_2(x, u) \cdot \overline{\partial}h_1(h_2(x)), \\ &\quad \overline{M}_{\mathcal{F}}h_2(x, u) \cdot \underline{\partial}h_1(h_2(x)), \\ &\quad \overline{M}_{\mathcal{F}}h_2(x, u) \cdot \overline{\partial}h_1(h_2(x)) \}. \quad (\text{A.3}) \end{aligned}$$

Since $L_{\mathcal{F}}h(x, u) \subseteq \mathbb{W}$, $\overline{M}_{\mathcal{F}}h(x, u) = \sup\{L_{\mathcal{F}}h(x, u)\} \leq \sup \mathbb{W}$ which then results in (9). If \mathcal{F} is a singleton, equality is obtained in every step in (A.3). Furthermore, if h_1 is regular and h_2 is continuously differentiable, then the quality in (A.1) holds and $L_{\mathcal{F}}h(x, u) = \mathbb{W}$ (Clarke, 1990). Therefore, $\overline{M}_{\mathcal{F}}h(x, u) = \sup\{L_{\mathcal{F}}h(x, u)\} = \sup \mathbb{W}$. \square

B Proof of Theorem 3.3

The proof is divided into two parts: the first part considers the case when $\lambda_i > 0$, $i \in [1, N]$, and the other part considers the case when $\lambda_i < 0$, $i \in [1, N]$.

1) $\lambda_i > 0$, $i \in [1, N]$: In this case, we aim to show that

$$\overline{M}_{\mathcal{F}}h(x, u) \leq \sum_{i=1}^N \lambda_i \overline{M}_{\mathcal{F}}h_i(x, u). \quad (\text{B.1})$$

To prove this, define the set \mathbb{W} as

$$\begin{aligned} \mathbb{W} &= \{\langle v, \xi \rangle \in \mathbb{R} \mid v \in \mathcal{F}(x, u), \xi \in \sum_{i=1}^N \lambda_i \partial h_i(x)\} \\ &= \{\langle v, \sum_{i=1}^N \lambda_i \xi_i \rangle \in \mathbb{R} \mid v \in \mathcal{F}(x, u), \xi_i \in \partial h_i(x)\} \\ &\subseteq \sum_{i=1}^N \lambda_i \{\langle v, \xi_i \rangle \in \mathbb{R} \mid v \in \mathcal{F}(x, u), \xi_i \in \partial h_i(x)\} \\ &= \sum_{i=1}^N \lambda_i L_{\mathcal{F}}h_i(x, u), \quad (\text{B.2}) \end{aligned}$$

where the equality holds if \mathcal{F} is a singleton. Since $\lambda_i > 0$, $i \in [1, N]$, taking the supremum of (B.2) yields

$$\sup \mathbb{W} \leq \sum_{i=1}^N \lambda_i (\sup L_{\mathcal{F}}h_i(x, u)) = \sum_{i=1}^N \lambda_i \overline{M}_{\mathcal{F}}h_i(x, u).$$

According to (Clarke, 1990, Corollary 2), we have

$$\partial h(x) \subseteq \sum_{i=1}^N \lambda_i \partial h_i(x). \quad (\text{B.3})$$

The equality holds if $h_i, i \in [1, N]$, are regular. This implies that $L_{\mathcal{F}}h(x, u) \subseteq \mathbb{W}$. Therefore, $\sup L_{\mathcal{F}}h(x, u) \leq \sup \mathbb{W}$ and $\overline{M}_{\mathcal{F}}h(x, u) \leq \sum_{i=1}^N \lambda_i \overline{M}_{\mathcal{F}}h_i(x, u)$.

2) $\lambda_i < 0, i \in [1, N]$: In this case, we aim to show that

$$\overline{M}_{\mathcal{F}}h(x, u) \leq \sum_{i=1}^N \lambda_i \underline{M}_{\mathcal{F}}h_i(x, u). \quad (\text{B.4})$$

The proof for this part follows directly from that of the first part, by noting that when a nonempty compact set is multiplied by a negative number λ_i , sup becomes inf.

Combining (B.1) and (B.4) leads to the result in (10). The claim of equality can be verified by observing that the equality holds in (B.2) if \mathcal{F} is a singleton, and also in (B.3) if h_i are regular and $\lambda_i > 0, i \in [1, N]$. \square

References

- Agarwal, A., Agrawal, R., Tayal, M., Jagtap, P., & Kothathaya, S. (2024). Real time safety of fixed-wing uavs using collision cone control barrier functions. *arXiv preprint arXiv:2407.19335*, .
- Alefeld, G., & Mayer, G. (2000). Interval analysis: theory and applications. *Journal of Computational and Applied Mathematics*, 121, 421–464.
- Ames, A. D., Coogan, S., Egerstedt, M., Notomista, G., Sreenath, K., & Tabuada, P. (2019). Control barrier functions: Theory and applications. In *18th European Control Conference* (pp. 3420–3431). IEEE.
- Ames, A. D., Xu, X., Grizzle, J. W., & Tabuada, P. (2016). Control barrier function based quadratic programs for safety critical systems. *IEEE Transactions on Automatic Control*, 62, 3861–3876.
- Artstein, Z. (1983). Stabilization with relaxed controls. *Nonlinear Analysis: Theory, Methods & Applications*, 7, 1163–1173.
- Braun, P., Grüne, L., & Kellett, C. M. (2021). (*In*) stability of differential inclusions: notions, equivalences, and Lyapunov-like characterizations. Springer Nature.
- Braun, P., & Kellett, C. M. (2017). On (the existence of) control lyapunov barrier functions. *Preprint*, <https://eref.uni-bayreuth.de/40899>, .
- Braun, P., & Kellett, C. M. (2020). Comment on “stabilization with guaranteed safety using control lyapunov–barrier function”. *Automatica*, 122, 109225.
- Braun, P., Kellett, C. M., & Zaccarian, L. (2019). Complete control lyapunov functions: Stability under state constraints. *IFAC-PapersOnLine*, 52, 358–363.
- Chen, S., & Fazlyab, M. (2024). Learning performance-oriented control barrier functions under complex safety constraints and limited actuation. *arXiv preprint arXiv:2401.05629*, .
- Chen, S., Molu, L., & Fazlyab, M. (2024). Verification-aided learning of neural network barrier functions with termination guarantees. *arXiv preprint arXiv:2403.07308*, .
- Clarke, F. H. (1990). *Optimization and nonsmooth analysis*. SIAM.
- Cortes, C. J., Clark, G., Coogan, S., & Thitsa, M. (2024). The mandalay derivative for nonsmooth systems: Applications to nonsmooth control barrier functions. *IEEE Control Systems Letters*, 8, 976–981.
- Dawson, C., Qin, Z., Gao, S., & Fan, C. (2022). Safe nonlinear control using robust neural lyapunov-barrier functions. In *Conference on Robot Learning* (pp. 1724–1735). PMLR.
- Du, D., Han, S., Qi, N., Ammar, H. B., Wang, J., & Pan, W. (2023). Reinforcement learning for safe robot control using control lyapunov barrier functions. In *IEEE International Conference on Robotics and Automation* (pp. 9442–9448). IEEE.
- Edwards, A., Peruffo, A., & Abate, A. (2023). A general verification framework for dynamical and control models via certificate synthesis. *arXiv preprint arXiv:2309.06090*, .
- Glotfelter, P., Cortés, J., & Egerstedt, M. (2017). Nonsmooth barrier functions with applications to multi-robot systems. *IEEE control systems letters*, 1, 310–315.
- Gomez, M. A., Cruz-Ancona, C. D., & Fridman, L. (2022). On the notion of safe sliding mode control. *arXiv preprint arXiv:2212.01847*, .
- Li, B., Wen, S., Yan, Z., Wen, G., & Huang, T. (2023). A survey on the control lyapunov function and control barrier function for nonlinear-affine control systems. *IEEE/CAA Journal of Automatica Sinica*, 10, 584–602.
- Liberzon, D. (2003). *Switching in systems and control* volume 190. Springer.
- Marley, M., Skjetne, R., & Teel, A. R. (2024). Hybrid control barrier functions for continuous-time systems. *IEEE Transactions on Automatic Control*, DOI: 10.1109/TAC.2024.3374265.
- Meng, Y., Li, Y., Fitzsimmons, M., & Liu, J. (2022). Smooth converse lyapunov-barrier theorems for asymptotic stability with safety constraints and reach-avoid-stay specifications. *Automatica*, 144, 110478.
- Mestres, P., & Cortés, J. (2024). Feasibility and regularity analysis of safe stabilizing controllers under uncertainty. *Automatica*, 167, 111800.
- Morcego, B., Yin, W., Boersma, S., van Henten, E., Puig, V., & Sun, C. (2023). Reinforcement learning versus model predictive control on greenhouse climate control. *Computers and Electronics in Agriculture*, 215, 108372.
- Romdlony, M. Z., & Jayawardhana, B. (2016). Stabilization with guaranteed safety using control lyapunov–barrier function. *Automatica*, 66, 39–47.
- Schneeberger, M., Mastellone, S., & Dörfler, F. (2024). Advanced safety filter based on SOS Control Bar-

- rier and Lyapunov Functions. *arXiv preprint arXiv:2401.06901*, .
- Sontag, E., & Sussmann, H. J. (1995). Nonsmooth control-lyapunov functions. In *Proceedings of 1995 34th IEEE conference on decision and control* (pp. 2799–2805). IEEE volume 3.
- Sontag, E., & Wang, Y. (2000). Lyapunov characterizations of input to output stability. *SIAM Journal on Control and Optimization*, *39*, 226–249.
- Sontag, E. D. (1989). A ‘universal’ construction of artstein’s theorem on nonlinear stabilization. *Systems & Control Letters*, *13*, 117–123.
- Wang, H., Margellos, K., & Papachristodoulou, A. (2024). Safe and stable filter design using a relaxed compatibility control barrier-lyapunov condition. *arXiv preprint arXiv:2407.00414*, .
- Wang, J., He, H., & Yu, J. (2020). Stabilization with guaranteed safety using barrier function and control lyapunov function. *Journal of the Franklin Institute*, *357*, 10472–10491.
- Wang, X., Knoedler, L., Mathiesen, F. B., & Alonso-Mora, J. (2023). Simultaneous synthesis and verification of neural control barrier functions through branch-and-bound verification-in-the-loop training. *arXiv preprint arXiv:2311.10438*, .
- Wu, Z., Albalawi, F., Zhang, Z., Zhang, J., Durand, H., & Christofides, P. D. (2019). Control lyapunov-barrier function-based model predictive control of nonlinear systems. *Automatica*, *109*, 108508.
- Xiao, W., Cassandras, C. G., & Belta, C. A. (2021). Bridging the gap between optimal trajectory planning and safety-critical control with applications to autonomous vehicles. *Automatica*, *129*, 109592.
- Yang, Y., Jiang, Y., Liu, Y., Chen, J., & Li, S. E. (2023). Model-free safe reinforcement learning through neural barrier certificate. *IEEE Robotics and Automation Letters*, *8*, 1295–1302.
- Zeng, D., Jiang, Y., Wang, Y., Zhang, H., & Feng, Y. (2023). Robust adaptive control barrier functions for input-affine systems: Application to uncertain manipulator safety constraints. *IEEE Control Systems Letters*, *8*, 279–284.
- Zhao, P., Ghabcheloo, R., Cheng, Y., Abdi, H., & Hovakimyan, N. (2023). Convex synthesis of control barrier functions under input constraints. *IEEE Control Systems Letters*, .
- Zheng, W., & Zhu, B. (2024). Control lyapunov-barrier function based model predictive control for stochastic nonlinear affine systems. *International Journal of Robust and Nonlinear Control*, *34*, 91–113.